

- Forster I. Conditional gene targeting in macrophages and granulocytes using LysMcre mice. *Transgenic Res.* 1999;8:265-277.
19. Suzuki A, Yamaguchi MT, Ohteki T, et al. T cell-specific loss of Pten leads to defects in central and peripheral tolerance. *Immunity.* 2001;14:523-534.
 20. Miyoshi H, Blomer U, Takahashi M, Gage FH, Verma IM. Development of a self-inactivating lentivirus vector. *J Virol.* 1998;72:8150-8157.
 21. Nagai T, Ibata K, Park ES, Kubota M, Mikoshiba K, Miyawaki A. A variant of yellow fluorescent protein with fast and efficient maturation for cell-biological applications. *Nat Biotechnol.* 2002;20:87-90.
 22. Suzue K, Kobayashi S, Takeuchi T, Suzuki M, Koyasu S. Critical role of dendritic cells in determining the Th1/Th2 balance and the disease outcome upon *Leishmania major* infection. *Int Immunol.* 2008;20:337-343.
 23. Cross DA, Alessi DR, Cohen P, Andjelkovich M, Hemmings BA. Inhibition of glycogen synthase kinase-3 by insulin mediated by protein kinase B. *Nature.* 1995;378:785-789.
 24. Guha M, Mackman N. The phosphatidylinositol 3-kinase-Akt pathway limits lipopolysaccharide activation of signaling pathways and expression of inflammatory mediators in human monocyte cells. *J Biol Chem.* 2002;277:32124-32132.
 25. Yu Y, Nagai S, Wu H, Neish AS, Koyasu S, Gewirtz AT. TLR5-mediated phosphoinositide 3-kinase activation negatively regulates flagellin-induced proinflammatory gene expression. *J Immunol.* 2006;176:6194-6201.
 26. Bierer BE, Mattila PS, Standaert RF, et al. Two distinct signal transmission pathways in T lymphocytes are inhibited by complexes formed between an immunophilin and either FK506 or rapamycin. *Proc Natl Acad Sci U S A.* 1990;87:9231-9235.
 27. Long X, Lin Y, Ortiz-Vega S, Yonezawa K, Avruch J. Rheb binds and regulates the mTOR kinase. *Curr Biol.* 2005;15:702-713.
 28. Moore KW, de Waal Malefyt R, Coffman RL, O'Garra A. Interleukin-10 and the interleukin-10 receptor. *Annu Rev Immunol.* 2001;19:683-765.
 29. Ding Y, Chen D, Tarcsafalvi A, Su R, Qin L, Bromberg JS. Suppressor of cytokine signaling 1 inhibits IL-10-mediated immune responses. *J Immunol.* 2003;170:1383-1391.
 30. Martin M, Rehani K, Jope RS, Michalek SM. Toll-like receptor-mediated cytokine production is differentially regulated by glycogen synthase kinase 3. *Nat Immunol.* 2005;6:777-784.
 31. Rodionova E, Conzelmann M, Maraskovsky E, et al. GSK-3 mediates differentiation and activation of proinflammatory dendritic cells. *Blood.* 2007;109:1584-1592.
 32. Mocellin S, Marincola FM, Young HA. Interleukin-10 and the immune response against cancer: a counterpoint. *J Leukoc Biol.* 2005;78:1043-1051.
 33. McGuirk P, McCann C, Mills KH. Pathogen-specific T regulatory 1 cells induced in the respiratory tract by a bacterial molecule that stimulates interleukin 10 production by dendritic cells: a novel strategy for evasion of protective T helper type 1 responses by *Bordetella pertussis*. *J Exp Med.* 2002;195:221-231.
 34. Akbari O, DeKruyff RH, Umetsu DT. Pulmonary dendritic cells producing IL-10 mediate tolerance induced by respiratory exposure to antigen. *Nat Immunol.* 2001;2:725-731.
 35. Lee YR, Yang IH, Lee YH, et al. Cyclosporin A and tacrolimus, but not rapamycin, inhibit MHC-restricted antigen presentation pathways in dendritic cells. *Blood.* 2005;105:3951-3955.
 36. Hackstein H, Tanser T, Zahorchak AF, et al. Rapamycin inhibits IL-4-induced dendritic cell maturation in vitro and dendritic cell mobilization and function in vivo. *Blood.* 2003;101:4457-4463.
 37. Foster DA. Regulation of mTOR by phosphatidic acid? *Cancer Res.* 2007;67:1-4.
 38. Puig-Kroger A, Relloso M, Fernandez-Capetillo O, et al. Extracellular signal-regulated protein kinase signaling pathway negatively regulates the phenotypic and functional maturation of monocyte-derived human dendritic cells. *Blood.* 2001;98:2175-2182.
 39. Kim AH, Khursigara G, Sun X, Franke TF, Chao MV. Akt phosphorylates and negatively regulates apoptosis signal-regulating kinase 1. *Mol Cell Biol.* 2001;21:893-901.
 40. Cao X, Wei G, Fang H, et al. The inositol 3-phosphatase PTEN negatively regulates Fc gamma receptor signaling, but supports Toll-like receptor 4 signaling in murine peritoneal macrophages. *J Immunol.* 2004;172:4851-4857.
 41. Park HS, Kim MS, Huh SH, et al. Akt (protein kinase B) negatively regulates SEK1 by means of protein phosphorylation. *J Biol Chem.* 2002;277:2573-2578.
 42. Utsugi M, Dobashi K, Ishizuka T, et al. c-Jun N-terminal kinase negatively regulates lipopolysaccharide-induced IL-12 production in human macrophages: role of mitogen-activated protein kinase in glutathione redox regulation of IL-12 production. *J Immunol.* 2003;171:628-635.
 43. Ma W, Gee K, Lim W, et al. Dexamethasone inhibits IL-12p40 production in lipopolysaccharide-stimulated human monocyte cells by down-regulating the activity of c-Jun N-terminal kinase, the activation protein-1, and NF-kappa B transcription factors. *J Immunol.* 2004;172:318-330.
 44. Gauthier G, Humbert M, Desauvieu F, et al. A type I interferon autocrine-paracrine loop is involved in Toll-like receptor-induced interleukin-12p70 secretion by dendritic cells. *J Exp Med.* 2005;201:1435-1446.
 45. Hoentjen F, Sartor RB, Ozaki M, Jobin C. STAT3 regulates NF-kappa B recruitment to the IL-12p40 promoter in dendritic cells. *Blood.* 2005;105:689-696.
 46. Jefferies HB, Fumagalli S, Dennis PB, Reinhard C, Pearson RB, Thomas G. Rapamycin suppresses 5' TOP mRNA translation through inhibition of p70s6k. *EMBO J.* 1997;16:3693-3704.
 47. Soliman GA. The mammalian target of rapamycin signaling network and gene regulation. *Curr Opin Lipidol.* 2005;16:317-323.
 48. Cunningham JT, Rodgers JT, Arlow DH, Vazquez F, Mootha VK, Puigserver P. mTOR controls mitochondrial oxidative function through a YY1-PGC-1alpha transcriptional complex. *Nature.* 2007;450:736-740.

A Novel GDP-dependent Pyruvate Kinase Isozyme from *Toxoplasma gondii* Localizes to Both the Apicoplast and the Mitochondrion*

Received for publication, November 2, 2007, and in revised form, March 3, 2008. Published, JBC Papers in Press, March 6, 2008, DOI 10.1074/jbc.M709015200

Tomoya Saito^{†1}, Manami Nishi^{§1}, Muoyi I. Lim[§], Bo Wu[§], Takuya Maeda[‡], Hisayuki Hashimoto[‡], Tsutomu Takeuchi[‡], David S. Roos^{§2}, and Takashi Asai^{†3}

From the [†]Department of Tropical Medicine and Parasitology, Keio University School of Medicine, 35 Shinanomachi, Shinjuku-ku, Tokyo 160-8582, Japan and the [§]Department of Biology, University of Pennsylvania, Philadelphia, Pennsylvania 19104

We previously reported a cytosolic pyruvate kinase (EC 2.7.1.40) from *Toxoplasma gondii* (TgPyKI) that differs from most eukaryotic pyruvate kinases in being regulated by glucose 6-phosphate rather than fructose 1,6-diphosphate. Another putative pyruvate kinase (TgPyKII) was identified from parasite genome, which exhibits 32% amino acid sequence identity to TgPyKI and retains pyruvate kinase signature motifs and amino acids essential for substrate binding and catalysis. Whereas TgPyKI is most closely related to plant/algal enzymes, phylogenetic analysis suggests a proteobacterial origin for TgPyKII. Enzymatic characterization of recombinant TgPyKII shows a high pH optimum at 8.5, and a preference for GDP as a phosphate recipient. Catalytic activity is independent of K⁺, and no allosteric or regulatory effects were observed in the presence of fructose 1,6-diphosphate, fructose 2,6-diphosphate, glucose 6-phosphate, ribose 5-phosphate, AMP, or ATP. Unlike TgPyKI, native TgPyKII activity was exclusively associated with the membranous fraction of a *T. gondii* tachyzoite lysate. TgPyKII possesses a long N-terminal extension containing five putative start codons before the conserved region and localizes to both apicoplast and mitochondrion by immunofluorescence assay using native antibody and fluorescent protein fusion to the N-terminal extension. Further deletion and site-directed mutagenesis suggests that a translation product from 1st Met is responsible for the localization to the apicoplast, whereas one from 3rd Met is for the mitochondrion. This is the first study of a potential mitochondrial pyruvate kinase in any system.

Toxoplasma gondii is an obligate intracellular protozoan parasite of warm-blooded animals, including humans (1). Although normally asymptomatic, toxoplasmosis is a significant problem in pregnant women infected early during gestation, immunocompromised individuals, and livestock. This parasite is a member of the phylum Apicomplexa, which includes many other parasites such as *Plasmodium* species responsible for malaria. Glucose is thought to be the main source of energy for the rapidly multiplying forms of both *Toxoplasma* and *Plasmodium*, which use the Embden-Meyerhof pathway for glycolytic phosphorylation (2).

Pyruvate kinase catalyzes the essentially irreversible transphosphorylation from phosphoenolpyruvate (PEP)⁴ to ADP-producing pyruvate (3). In most mammals and bacteria, pyruvate kinase is allosterically regulated by fructose 1,6-diphosphate (4) and thus plays a regulatory role in glycolysis. The product pyruvate feeds into many metabolic pathways, placing pyruvate kinase at a crucial metabolic intersection. Many organisms express multiple pyruvate kinase isozymes with different kinetic properties. For example, *Escherichia coli* bears two isozymes, type I and II, both of which are homotropically activated by the substrate PEP. The type I isozyme is also activated heterotropically by fructose 1,6-diphosphate and is inhibited by ATP (5), whereas the type II isozyme is activated by AMP and monophosphorylated sugars (6). Pyruvate kinases are expressed in the cytosol in most organisms. Plants and algae have additional isozymes in chloroplasts with markedly different physical and kinetic/regulatory characteristics (7).

We have previously described the kinetic and regulatory properties of the cytosolic *T. gondii* pyruvate kinase (TgPyKI). Unlike *T. gondii* hexokinase (8) and phosphofructokinase (9) that lack allosteric regulation, TgPyKI is allosterically regulated by glucose 6-phosphate (10, 11), suggesting an important role in the control of glycolysis. We recently identified a second,

* This work was supported, in whole or in part, by National Institutes of Health grants. This work was also supported by Grant-in-aid for Scientific Research (KAKENHI) for Young Scientists (B) from the Ministry of Education, Culture, Sports, Science, and Technology 15790217, a Keio University grant-in-aid for encouragement of young medical scientists, and a Keio University special grant-in-aid for innovative collaborative research projects. The costs of publication of this article were defrayed in part by the payment of page charges. This article must therefore be hereby marked "advertisement" in accordance with 18 U.S.C. Section 1734 solely to indicate this fact.

The nucleotide sequence(s) reported in this paper has been submitted to the GenBank™/EBI Data Bank with accession number(s) AB118155.

¹ Both authors contributed equally to this work.

² Senior Scholar in Global Infectious Diseases of the Ellison Medical Foundation.

³ To whom correspondence should be addressed: Dept. of Tropical Medicine and Parasitology, Keio University School of Medicine, 35 Shinanomachi, Shinjuku-ku, Tokyo 160-8582, Japan. Tel.: 81-3-3353-1211 (Ext. 62747); Fax: 81-3-3353-5958; E-mail: asait@sc.itc.keio.ac.jp.

⁴ The abbreviations used are: PEP, phosphoenolpyruvate; ACP, acyl carrier protein; TgPyK, *T. gondii* pyruvate kinase; YFP, yellow fluorescent protein; SA, predicted signal anchor; SP, signal peptide; pTP, predicted plastid transit peptide; mTP, predicted mitochondrion targeting peptide; aa, amino acid; CHES, 2-(cyclohexylamino)ethanesulfonic acid; bis-Tris, 2-[bis(2-hydroxyethyl)amino]-2-(hydroxymethyl)propane-1,3-diol; MOPS, 4-morpholinepropanesulfonic acid; PBS, phosphate-buffered saline; Ab, antibody; HA, hemagglutinin; MES, 2-(N-morpholino)ethanesulfonic acid; HFF, human foreskin fibroblast; IFA, immunofluorescence assay; ER, endoplasmic reticulum; TES, 2-[2-hydroxy-1,1-bis(hydroxymethyl)ethyl]amino]ethanesulfonic acid; NDP, nucleoside diphosphate; RFP, red fluorescent protein.

Novel Pyruvate Kinase in Two Organelles in *T. gondii*

highly diverged isozyme in *T. gondii* EST and genome data bases (12, 13). This study describes the molecular genetic characterization, phylogeny, recombinant expression/purification, kinetic characterization, and subcellular localization of this *T. gondii* pyruvate kinase isozyme (TgPykII).

EXPERIMENTAL PROCEDURES

Parasites, Host Cells, Chemicals, and Reagents—RH strain *T. gondii* tachyzoites were maintained by serial passage in primary human foreskin fibroblasts (HFF) in Eagle's minimum essential media (Invitrogen) containing 1% heat-inactivated fetal bovine serum (Ed1 media) (14) or in mouse peritoneal fluid (15). Construction of parasites stably expressing *ptubFNR*_L-yellow fluorescent protein (YFP)-HA (labeling the apicoplast) and *ptubHSP60*_L-RFP (labeling the mitochondrion) is described elsewhere (16). PEP, phosphorylated sugars, nucleotides, potassium ferricyanide, and amino acids were obtained from Sigma. Rabbit polyclonal anti-acyl carrier protein (ACP) antibody was kindly provided by Drs. G. I. McFadden and R. F. Waller (17). MitoTrackerRed CMXRos (8-(4'-chloromethyl) phenyl-2,3,5,6,11,12,14,15-octa-hydro-1H,4H,10H,13H-diquinolizino-8H-xanthylum chloride), and Alexa Fluor Marina Blue/361 and 594-conjugated goat anti-rabbit antibodies were obtained from Invitrogen.

Cloning and Sequencing of TgPykII cDNA—The following PCR primers were designed based on *T. gondii* ESTs CB030989, CB030879, and B1921053 (8): 5'-TGCAGAAATCGTCGCG-CCGACGCG-3' (sense) and 5'-GCCGTGCTTGCCTTCTT-TGG-3' (antisense). PCR amplification of a *T. gondii* RH tachyzoite λ ZAP-II cDNA library (kindly provided by Dr. J. Ajioka, Cambridge University, UK) yielded a product with the expected size of 371 bp, which was used as a probe for cDNA library screening (8). Positive clones were sequenced on both strands using a Genetic Analyzer model 310 and 3700 (Applied Biosystems, Tokyo, Japan). The composite cDNA sequence was used for BLAST query against ToxoDB (18) to identify gene model TgTigrScan_6611. To confirm the 5' end of the TgPykII cDNA, total RNA was extracted from RH strain of *T. gondii* tachyzoites (RNAqueous, Ambion, TX), and cDNA was amplified using GeneRacer kit (Invitrogen). 5'-rapid amplification of cDNA ends was performed using a gene-specific primer 5'-CACGTAGACAGAGGTGACGCTTCGGGG-3'. The complete cDNA sequence was analyzed by VectorNTI software (Informax, Bethesda). The protein domains, families, and functional sites were analyzed using PROSITE (19). Signal properties were analyzed using TargetP (20, 21), SignalP (21, 22), and ChloroP (23) softwares. Hydrophobicity was examined using the Kyte and Doolittle procedure (24).

Phylogenetic Analysis—Twenty nine pyruvate kinase sequences from 20 taxa were extracted from GenBankTM and the OrthoMCL data base (25, 26) (see Fig. 2 legend for GenBankTM accession number), and aligned using ClustalX 1.83 (27), with manual curation. Regions of uncertain alignment were omitted, leaving 333 amino acid positions for analysis. Maximum likelihood trees were constructed using PROML from the PHYLIP 3.6a3 package (28), with 100 replicates, global rearrangement, and randomized input order options in conjunction with estimated parameter γ and the proportion of invariable sites obtained from TREE-PUZZLE5.1 (29). Bayesian

analysis (30, 31) was carried out using MrBayes 3.0 with the JTT amino acid substitution model and 200,000 search generations.

Expression and Purification of Recombinant TgPykII—An open reading frame predicted to encode the conserved region (from amino acid 293 to 988) of TgPykII was amplified using primers 5'-TACGGATCCCTCTCTGCTGCGTCGCCC-3' (sense) and 5'-TCGGGATCCCTATCGCCCTGACTCGAG-AGT-3' (antisense), and cloned into the BamHI site of vector pGEX-6p-1 (Amersham Biosciences). Expression of the glutathione S-transferase-TgPykII-(293-988) fusion protein in *E. coli* BL21 was induced with 0.5 mM isopropyl β -thiogalactoside for 2.5 h, and purification of recombinant TgPykII was carried out by affinity chromatography on glutathione-Sepharose 4B (Amersham Biosciences), followed by treatment with Pre-Scission Protease (Amersham Biosciences). The protein was applied to a DEAE-Toyo Pearl 650s column (TOSOH, Tokyo, Japan) equilibrated with 10 mM Tris-Cl, pH 8.0, containing 1 mM EDTA. Peak fractions eluted with a linear 0-500 mM gradient of KCl were pooled, concentrated, assayed for purity and concentration, and stored in 30% glycerol (w/v) at -80 °C. The protein concentration was determined by the dye-binding procedure described by Bradford (32) using bovine serum albumin as a standard. The purity of recombinant pyruvate kinase was analyzed by electrophoresis on 5-10% acrylamide gel. The protein was detected by Coomassie Brilliant Blue R-250 staining.

Enzyme Assays—Pyruvate kinase activity was determined by lactate dehydrogenase-coupled spectrophotometric assay (32), whereas monitoring oxidation of NADH due to pyruvate reduction at 340 nm was by using a UV-1600 spectrophotometer equipped with a TCC-240A temperature-controlled cell (Shimadzu Co, Kyoto, Japan). 1-ml standard reaction mixture for assaying TgPykII activity contained 1 mM PEP, 0.5 mM GDP, 25.5 mM MgCl₂, 0.2 mM NADH, 20 units of rabbit muscle lactate dehydrogenase type II (Sigma), 100 mM Tris-Cl, pH 8.5, and 10-20 ng of the test enzyme. For substrate specificity studies, MgCl₂ was added in 25 mM excess of NDP to ensure formation of the MgNDP²⁻ complex. All reactions were initiated by the addition of the substrate NDP. For determining optimal pH of recombinant TgPykII, MES, Tris-Cl, or CHES/NaOH buffers were used to generate a pH range from 6.0 to 10.0. Activities of TgPykI and succinate dehydrogenase were assayed as described previously (10, 11). All assays were carried out in triplicate at 37 °C. Reactions were monitored for 5 min, and the initial velocity was calculated from a tangent fitted to the reaction curve. Kinetic data were calculated using a nonlinear curve fitting algorithm (SigmaPlot 2000 software; SPSS Inc., Chicago).

Subcellular Fractionation of *T. gondii* Tachyzoites—10¹⁰ tachyzoites were washed twice and resuspended in TES homogenization buffer (250 mM sucrose, 1 mM EDTA, 5 mM triethanolamine-HCl, pH 7.5) and disrupted by French press at 35 kg/cm². After sedimentation of unbroken cells (~10%) at 2250 \times g for 10 min, the supernatant was centrifuged for 20 min at 20,000 \times g to yield a cytosolic (supernatant) and membranous (pellet) fractions. The pellet was washed once, resuspended in 1% Triton X-100 in TES buffer, and mechanically homogenized using a polychlorotrifluoroethylene homogenizer.

Native Antibody Production and Immunoblotting—Recombinant TgPyKII-(293–988) purified from *E. coli* was used to immunize New Zealand White rabbits. Following three 50- μ g injections at 2-week intervals, whole IgG was isolated from serum, and anti-TgPyKII IgG was affinity-purified using CNBr-activated Sepharose 4B (Amersham Biosciences), which couples recombinant TgPyKII-(293–988) as described previously (33). To check the cross-reactivity of anti-TgPyKII to TgPyKI, 3 ng of recombinant TgPyKI (11) and recombinant TgPyKII were loaded on 8% gradient polyacrylamide gel, which was then transferred to a Nitrocellulose Hybond-C extra membrane (Amersham Biosciences) using a semidry blotting apparatus. The membrane was blocked for 20 min with 2% skimmed milk in phosphate-buffered saline (PBS) containing 0.2% Tween 20 and incubated for 1 h with anti-TgPyKII antibody (1:25 in blocking solution). Following washes in PBS with 0.2% Tween 20, the membrane was incubated with alkaline phosphatase goat anti-rabbit IgG (1:3000) (Vector Laboratories) for 1 h, following detection with a 5-bromo-4-chloro-3-indolyl phosphate-nitro blue tetrazolium system (Roche Applied Science). The molecular sizes of protein bands were determined with reference to pre-stained SDS-gel electrophoresis standards (Bio-Rad). To detect endogenous TgPyKII expressed in *T. gondii*, 10⁸ RH tachyzoites released from HFF monolayer were filtered through 3- μ m pore-size Nuclepore polycarbonate filters (Whatman) and pelleted by centrifugation at 900 \times g for 12 min. Parasites were lysed in PBS, containing NuPAGE LDS sample buffer (Invitrogen) and 0.5 M dithiothreitol. After denaturation at 70 °C for 10 min, parasite lysates were loaded on bis-Tris, 4–12% polyacrylamide gels (Invitrogen), and protein gel electrophoresis was performed using NuPAGE system with MOPS/SDS running buffer (Invitrogen). Proteins were transferred to nitrocellulose membrane using a Trans-Blot SemiDry apparatus (Bio-Rad), which was then blocked with 5% nonfat dry milk and 3% fetal bovine serum in PBS. The membrane was incubated for 1 h with a rabbit anti-TgPyKII Ab (1:25 dilution) in blocking solution containing 0.2% Tween 20 (Sigma). Following washes in PBS with 0.2% Tween 20, the membrane was incubated for 1 h with a horseradish peroxidase-conjugated goat anti-rabbit secondary antibody (Bio-Rad) (1:2500 dilution) in blocking solution containing 0.2% Tween 20. Chemiluminescence reaction was performed using ECL Western blotting detection reagents (Amersham Biosciences), and blots were exposed on Kodak BioMax film.

Plasmid Construction—N-terminal 357 amino acids of TgPyKII (unconserved region containing five possible start codons) from 1st Met were amplified from a *T. gondii* RH cDNA using primers (note that restriction enzyme site is underlined and start codon is boldface) 5'-CATCGCAGATCTATGG-ACGATGGTGGAGCAGAGT-3' (sense) and 5'-CGTCACAC-TAGTCGGTCCGATGGTTGC-3' (antisense) and subcloned into BglII/AvrII sites of the *T. gondii* expression vector *ptub* or *pminPT_F*-YFP-HA (16)⁵ to produce *ptub/pminTgPyKII1stM*-(1–357)-YFP-HA. DNA fragments from each downstream four start codons were generated using *ptub/pminTgPyKII1stM*-(1–357)-

YFP-HA as a template, the above antisense primer, and the following sense primers: 5'-CATCGCAGATCTATGAACTTTCCAA-CTTGT-3' (from 2nd Met); 5'-CATCGCAGATCTATGGCGC-CTCTCCGACCC-3' (from 3rd Met); 5'-CATCGCAGATCTA-TGGATTTTCCACGGGTG-3' (from 4th Met); or 5'-CATCGC-AGATCTATGCTCTGCTGCGTCCG-3' (from 5th Met). Plasmids *ptub/pminTgPyKII2ndM*-(19–357)-YFP-HA, *ptub/pminTgPyKII3rdM*-(93–357)-YFP-HA, *ptub/pminTgPyKII4thM*-(122–357)-YFP-HA, and *ptub/pminTgPyKII5thM*-(293–357)-YFP-HA were constructed using above described subcloning method. To introduce a point mutation, methionine to alanine, at 2nd or 3rd Met, site-directed mutagenesis was performed using QuikChange site-directed mutagenesis kit (Stratagene, CA). The plasmid *ptub/pminTgPyKII1stM*-(1–357)-YFP-HA was used as a template in the PCR by utilizing the following sets of primers (mutated amino acids are lowercase): 5'-GCTAATGGTTTTGC-CAGCgcGAACTTTCCAATTGTGG-3' and 5'-CCACAAGT-TGGAAAGTTCgcGCTGGCAAACCATAGC-3' to produce *ptub/minTgPyKII[2ndM19A]*-YFP-HA, and 5'-CTCCTTCTCT-CCGCGgcGGCGCCTCTCCGACC-3' and 5'-GGTCGGAG-AGGCGCCgcCGCGGAGAGAAGGAG-3' to produce *ptub/minTgPyKII[3rdM93A]*-YFP-HA.

Parasite Transfection, Immunofluorescence Assay, and Fluorescent Microscopy—Parasite transfection was performed by electroporation as described previously (14). Parasites were inoculated onto glass coverslips (22 mm in diameter) with a confluent monolayer of HFF cells and incubated in a humidified 37 °C incubator for 24 h. Following a wash with PBS, coverslips were fixed with 3.7% paraformaldehyde in PBS, pH 7.0, for 5 min, permeabilized with 0.25% Triton X-100 in PBS, pH 7.0, for 10 min, and blocked for 30 min in a blocking solution (3% bovine serum albumin (fraction V, Fisher) and 5% fetal bovine serum in PBS, pH 7.0). For MitoTracker labeling, coverslips were incubated with 150 nM MitoTrackerRed CMXRos (Invitrogen) for 30 min and washed twice with Ed1 media before fixation. For immunofluorescence assay (IFA), coverslips were incubated with primary antibodies (anti-TgPyKII Ab at 1:25 dilution or anti-ACP Ab at a 1:2000 dilution in blocking solution) for 1 h. Coverslips were washed three times with 0.25% Triton X-100 in PBS, and primary antibodies were detected either with Alexa Fluor Marina Blue/361-conjugated (1:500 dilution) or 594-conjugated goat anti-rabbit antibodies (1:4000 dilution) (Invitrogen) in the blocking solution for 1 h. After two washes with 0.25% Triton X-100 in PBS and a wash with PBS, the coverslips were mounted on glass slides using Fluoromount-G (SouthernBiotech, AL). To find out the localization of endogenous TgPyKII, parasites stably expressing FNR₂-YFP-HA were labeled with MitoTracker Red CMXRos and subjected to IFA using anti-TgPyKII and Alexa Fluor Marina Blue/361-conjugated goat anti-rabbit antibodies (Invitrogen). For examination of deletion constructs, wild type RH parasites were transfected, labeled with MitoTracker Red CMXRos, and subjected to IFA with anti-ACP and Alexa Fluor Marina Blue/361-conjugated goat anti-rabbit antibodies. Point mutational constructs were transfected either to wild type RH parasites that are subsequently labeled with anti-ACP and Alexa Fluor 594-conjugated goat anti-rabbit antibodies (Invitrogen) or to parasites stably expressing *ptubHSP60_L*-RFP.

⁵ M. Nishi, C. He, O. Harb, J. Murray, and D. Roos, manuscript in preparation.

Stacked images were collected using an Olympus IX70 inverted microscope equipped with a 100-watt Hg-vapor lamp with appropriate barrier/emission filters. Images were captured with a CoolSNAP Hi Res CCD camera (Photometrics, AZ) and DeltaVision softWoRx software (Applied Precision, WA). All images were subjected to three-dimensional rendering using DeltaVision softWoRx.

RESULTS

Gene Organization, Functional Motifs, and Phylogenetic Analysis of *TgPyKII*—We cloned a second pyruvate kinase isozyme gene from *T. gondii*, *TgPyKII*, using EST data bases, cDNA library screening, and rapid amplification of cDNA ends. A BLAST search of the cDNA sequence in ToxoDB (18) identified the gene model *TgTigrScan_6611* in chromosome III, consisting of two exons (1092 and 1871 bp) and an intron (764 bp) that encodes 988 amino acids with a calculated molecular mass of 106,837 Da and a pI of 8.77. BLASTP search shows that *TgPyKII* is highly homologous to pyruvate kinases from α -proteobacteria with >40% identity and >50% similarity. Multiple sequence alignments with crystallized pyruvate kinases (35–37) show that *TgPyKII* has a long N-terminal extension before the conserved region beginning at aa 345 (Fig. 1).

Compared with the pyruvate kinase domain structure consisting of A₁, A₂, B, and C domains, three unique insertions in the middle of domain B, A₂, and C (37), are present (Fig. 1). Both *TgPyKI* and *TgPyKII* contain a pyruvate kinase signature (PROSITE; PS00110) (Fig. 1, line) as well as consensus motifs for pyruvate kinase, including binding sites of ADP, PEP, and divalent cations (Fig. 1, a, p, d, respectively). *TgPyKI* possesses all the conserved monovalent cation-binding sites (Fig. 1, m). In contrast, in *TgPyKII*, two binding sites Thr¹¹³ and Glu¹¹⁷ in *Felis catus* pyruvate kinase are substituted by Leu⁴¹² and Lys⁴¹⁶, respectively. These substitutions are a common feature of monovalent cation-independent pyruvate kinases (38–40). Furthermore, the presence of Glu⁸⁶⁸ in *TgPyKII*, conserved among enzymes that are insensitive to the pyruvate kinase activator, fructose 1,6-diphosphate (39), suggests that *TgPyKII* is not activated by fructose 1,6-diphosphate.

TgPyKII has overall amino acid sequence identity of 32% to *TgPyKI*. Unlike *TgPyKII*, *TgPyKI* shows high homology to pyruvate kinases in other apicomplexan parasites and plants. Phylogenetic tree indicates that *TgPyKI* is closely related to plant cytosolic pyruvate kinases along with pyruvate kinases from apicomplexan parasites such as *Cryptosporidium parvum* (EAK88569), *Plasmodium falciparum* (CAG25081), and *Theileria parva* (529.m04777) (Fig. 2). In contrast, *TgPyKII* clusters with proteobacteria pyruvate kinases, along with two isozymes from apicomplexan parasites *P. falciparum* (AAG35560) and *T. parva* (529.m04771) (Fig. 2). These results suggest a different evolutionary origin of the two isozymes in *T. gondii*, a probable

plant/algal origin of *TgPyKI* and a probably proteobacterial origin of *TgPyKII*.

Enzymatic Activity of Recombinant and Native *TgPyKII* Proteins—Conserved region of *TgPyKII* (*TgPyKII*-(293–988)) was expressed in *E. coli* as a fusion protein with glutathione S-transferase, which was removed by PreScission protease (Amersham Biosciences) digestion. SDS-PAGE detected the predicted size of 77 kDa for purified recombinant protein (Fig. 3A). The purified recombinant protein is shown to catalyze the pyruvate kinase reaction. The pH optimum of *TgPyKII* activity is at pH 8.5, and more than 80% of the maximal activity is observed between pH 8.0 and pH 9.5 (data not shown). At pH 7.0, the optimal pH of *TgPyKI* (11), the activity of *TgPyKII* is 50% of the maximal activity. The enzyme was stable when stored in buffer containing 20 mM Tris-Cl, pH 7.0, and 30% glycerol for 1 week at 4 °C. The enzyme activity remained stable after one freeze-thaw cycle.

Most pyruvate kinases require monovalent cations, show allosteric properties for PEP binding, and are regulated by phosphorylated sugars. Interestingly, amino acid sequence (Fig. 1) suggests that monovalent cations are not required for *TgPyKII* activity, which was confirmed by biochemical assay. Also, the saturation curve is hyperbolic with the substrate PEP. The K_m value for PEP is 0.116 ± 0.011 mM. Although most pyruvate kinases prefer ADP as a phosphate recipient, the k_{cat}/K_m values for GDP and IDP are 337- and 114-fold higher, respectively, than that for ADP (Table 1). Moreover, the substrates GDP and IDP exert inhibitory activities (Table 1). The specific activity at 0.5 mM CDP and UDP was less than 10% that at 0.5 mM GDP. These data indicate that GDP is a preferred substrate for *TgPyKII*. Other possible effectors were tested at sub-saturating concentrations of PEP and GDP (0.2 and 0.1 mM, respectively). None of the following compounds influence *TgPyKII* activity: fructose 1,6-diphosphate, glucose 6-phosphate, fructose 6-phosphate, glucose 1-phosphate, ribose 5-phosphate, ATP, ITP, AMP, His, Ser, Ala, Glu, Gln, Thr, Met, Gly, Ile, Asn, Cys, Pro, Arg, Lys, Phe, Trp, Leu, Asp, Val (1 mM each), Tyr (0.5 mM), 0.1 mM acetyl-CoA. Only 0.1 mM GTP reduces the V_{max} by $10 \pm 1\%$.

To examine native *TgPyKII* activity, we performed subcellular fractions of *T. gondii* tachyzoite cells. *TgPyKI* and -II activities were distinguished based on their pH optimum (7.0 versus 8.5, respectively), requirement for the monovalent cation, and phosphate recipient specificity (ADP versus GDP) (Table 2). As *TgPyKI* requires K⁺ for the activity, *TgPyKI* does not show any activity in the standard assay condition for *TgPyKII* lacking K⁺. In the standard assay condition for *TgPyKI*, *TgPyKII* shows less than 1/100 of its *TgPyKII* activity. Although *TgPyKI* activity is detected only in cytosolic fractions as reported previously (10), *TgPyKII* activity is exclusively associated with membranous

FIGURE 1. Amino acid sequence alignment of *T. gondii* pyruvate kinase II with four pyruvate kinases from other species. Accession numbers for the sequence data shown are as follows: *Tg2*, *T. gondii* isozyme II (this study; AB118155); *Pf2*, *P. falciparum* isozymes II (AAN35560); *Tp2*, *T. parva* isozyme II (529.m04771); *Tg1*, *T. gondii* isozymes I (BAB47171); *FsM1*, *F. catus* isozyme M1 (P11979). Identical residues are highlighted in black. Vertical lines indicate the dividing line of four three-dimensional domains (N, A1, A2, B, C) of pyruvate kinase as described previously (37). A horizontal line indicates the pyruvate kinase signature sequence (PROSITE, PS00110; p indicates PEP-binding sites; a indicates ADP-binding sites; d indicates divalent cation-binding sites; m indicates monovalent cation-binding sites; dashes indicate gaps in the alignment.

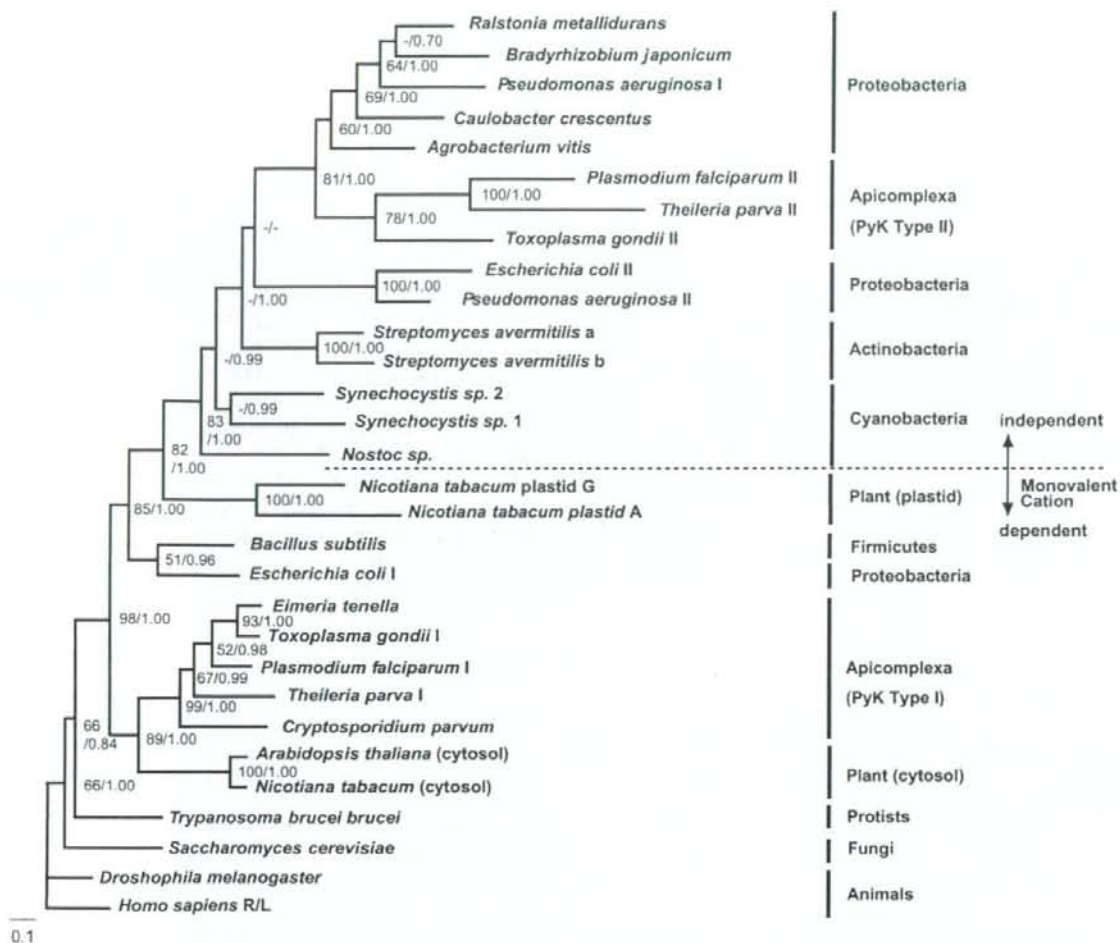


FIGURE 2. Phylogenetic tree of pyruvate kinase constructed based on the deduced amino acid sequences of pyruvate kinase genes of 20 taxa. Only evolutionarily conserved alignment regions (~230 amino acid characters) were used for phylogenetic inference by the Bayesian inference and maximum likelihood methods. The tree shown is the consensus tree estimated by Bayesian analysis with the JTT matrix. Maximum likelihood distance tree was also carried out. Numbers at branches are bootstrap values for the maximum likelihood protein distance analysis (100 replicates, >50 were indicated) and Bayesian posterior probabilities (>0.5 were indicated). Bar indicates the substitution. The accession numbers in GenBank™ for all pyruvate kinase sequences used for phylogenetic analysis are as follows: *Drosophila melanogaster* (AAC16244); *Homo sapiens* R/L (AAA60104); *Saccharomyces cerevisiae* (CAA32573); *Trypanosoma brucei brucei* (P30615); *C. parvum* (EAK88569); *P. falciparum* (I, CAG25081; II, AAN35560); *T. gondii* (I, BAB47171; II, in this article); *T. parva* (I, S29.m04777; II, S29.m04771); *A. thaliana* (cytosol, BAB10006); *Nicotiana tabacum* (cytosol, CAA82628; plastid A, CAA82222; plastid G, CAA82223); *Streptomyces avermitilis* (a, BAC70536; b, BAC73928); *Synechocystis* sp. (1, BAA10621; 2, BAA17574); *Nostoc* sp. PCC7120 (BAB74263); *Bacillus subtilis* (P80885); *E. coli* (type I, AAA24392; type II, AAA24473); *Pseudomonas aeruginosa* (I, NP_250189; II, NP_253019); *Bradyrhizobium japonicum* (NP_773778); *Ralstonia metallidurans* (ZP_00275735); *Caulobacter crescentus* (NP_420856); and *Agrobacterium vitis* (Q44473).

fraction, the purity of which is confirmed by mitochondrial succinate dehydrogenase activity. The procedure of solubilization of membranous fraction did not have any detrimental impact on the activity of recombinant TgPyKII. Thus, TgPyKII is localized to membrane-bound compartments.

Localization of TgPyKII and Analysis of Its Subcellular Localization Signals—Anti-TgPyKII antibody was generated to detect endogenous TgPyKII protein in *T. gondii* tachyzoite cells. Western blot analysis shows that anti-TgPyKII antibody specifically detects the recombinant TgPyKII protein (Fig. 3B, lane 1), not the recombinant TgPyKI protein (Fig. 3B, lane 2) and the host cell (data not shown). A single band of ~75 kDa was detected by this antibody in whole lysate of tachyzoite cells

(Fig. 3C). To analyze the localization of native TgPyKII protein in tachyzoite cells, FNR_L-YFP-HA parasites (labeling the apicoplast) were labeled with MitoTracker Red (labeling the mitochondrion) and TgPyKII antibody (Fig. 4). Endogenous TgPyKII (Fig. 4, blue) localizes to the apicoplast (Fig. 4, green) and the mitochondrion (Fig. 4, red) along with apical side of endoplasmic reticulum (ER) (Fig. 4, arrowheads), which was confirmed with a co-localization experiment using ER marker (data not shown).

Multiple sequence alignments of pyruvate kinases (Fig. 1) show that TgPyKII has a long N-terminal unconserved extension containing five possible start codons (Fig. 5A, red bold), which may acts as subcellular localization signal(s). TargetP,

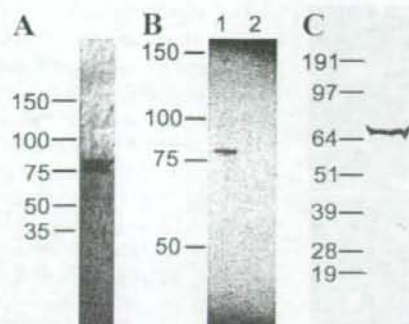


FIGURE 3. Recombinant protein expression and native antibody of *TgPyKII*. A, SDS-PAGE of 3 μ g of purified recombinant *TgPyKII* with the N-terminal extension truncated. Electrophoresis was carried out on 5–10% gradient polyacrylamide gel. The protein was detected by Coomassie Brilliant Blue R-250 staining. B and C, specificity of anti-*TgPyKII* IgG shown by Western blot analysis. B, 3 ng of recombinant *TgPyKII* (lane 1) and *TgPyKII* (lane 2). C, 1×10^8 *T. gondii* tachyzoite whole cell lysate. Molecular mass is expressed in kDa.

TABLE 1

Kinetic parameters of *T. gondii* pyruvate kinase I and II for nucleoside diphosphates

Substrate	Enzyme	K_m mM	K_i^a mM	k_{cat}^b s^{-1}	k_{cat}/K_m $mM^{-1} s^{-1}$
ADP	<i>TgPyKI</i> ^c	0.180 \pm 0.110		174	966
	<i>TgPyKII</i> ^d	7.99 \pm 0.44		47.6 \pm 1.4	6
GDP ^e	<i>TgPyKII</i>	0.0544 \pm 0.0061	1.68 \pm 0.18	110 \pm 4	2020
IDP ^f	<i>TgPyKII</i>	0.193 \pm 0.014	4.89 \pm 0.49	131 \pm 4	681

^a GDP and IDP exhibited substrate inhibition.

^b k_{cat} values were calculated as V_{max} divided by molar enzyme concentration.

^c Cited and calculated from data in Maeda *et al.* (11).

^d ADP concentration assayed was 1 to 10 mM.

^e GDP concentration assayed was 0.025 to 2 mM.

^f IDP concentration assayed was 0.05 to 4 mM.

TABLE 2

Total activity of enzymes in subcellular fractions of *T. gondii* tachyzoites

Fraction	Total activity ^a (units/10 ¹⁰ tachyzoite cells)		
	Pyruvate kinase activity		SDH ^d
	<i>TgPyKI</i> ^b	<i>TgPyKII</i> ^c	
Cytosolic fraction	153 \pm 7	<0.01	<0.005
Membranous fraction	<0.01	0.920 \pm 0.190	0.854 \pm 0.088

^a All values were determined by three independent experiments. One unit of enzyme activity is defined as the amount of enzyme resulting in the consumption of 1 μ mol of NADH/min (pyruvate kinase) or 2 μ mol of ferricyanide/min (succinate dehydrogenase).

^b Shown is the activity under optimal conditions and substrate for *T. gondii* pyruvate kinase I (1 mM PEP, 1 mM ADP, 10 mM MgSO₄, 100 mM KCl₂, pH 7.0).

^c Shown is the activity under optimal conditions and substrate for *T. gondii* pyruvate kinase II (1 mM PEP, 0.5 mM GDP, 25.5 mM MgCl₂, pH 8.5).

^d SDH means succinate dehydrogenase.

SignalP, and ChloroP were used to predict the presence of signals in N-terminal 357 amino acids (Fig. 5). SignalP 3.0 (21) with 100 truncation max residues was used to predict the presence of canonical secretory signal peptide (SP) or anchor (SA) in translation products from five possible start codons (Fig. 5, *ocher*). Although SignalP-NN, the neural networks based algorithm, predicted a weak SP cleavage site between aa 92 and 93 for the 1st Met protein product, SignalP-HMM (41), the hidden Markov model algorithm, highly favors SA ($p = 0.995$). The same prediction was observed for the 2nd Met product. The Kyte-Doolittle hydrophobicity profile showed the presence of a

strong hydrophobic stretch between aa -75 and 92 corresponding the prediction of SignalP (Fig. 5B). ChloroP (23) predicted possible plastid transit peptides (pTPs) for translation products from the 1st, 3rd, and 5th Met (Fig. 5, *green*). The predicted pTP cleavage sites for the 1st, 3rd, and 5th Met products are between aa 69 and 70, aa 159 and 160, and aa 309 and 310, respectively (note that amino acid positions are counted from the position of 1st Met). TargetP (20) predicted the presence of mitochondrial targeting peptides (mTPs) for translation products from 3rd, 4th, and 5th Met (Fig. 5, *magenta*). The predicted mTP cleavage sites are between aa 140 and 141 for the 3rd and 4th Met products and aa 316 to 317 for the 5th Met product. Summary of the possible signal sequences for various protein products is shown in Fig. 5C.

To determine whether the N-terminal unconserved region of *TgPyKII* can function as a dual targeting signal to the mitochondrion and the apicoplast, YFP-HA was fused to the N-terminal 357 aa of *TgPyKII* (*TgPyKII*1stM-(1–357)-YFP-HA) and expressed in tachyzoites (Fig. 6A). YFP labeling co-localizes to both the apicoplast (Fig. 5A, *blue*) and the mitochondrion (Fig. 5A, *red*), suggesting that this region is responsible for proper localization of *TgPyKII*. Because this N-terminal extension contains five possible start codons, the dual targeting of *TgPyKII*1stM-(1–357)-YFP-HA could result from one protein targeted to both organelles or two proteins targeted to each individual organelle. To answer this, we fused YFP-HA to N-terminal unconserved regions starting from downstream possible start codons (at aa positions 19 for 2nd Met, 93 for 3rd Met, 122 for 4th Met, and 293 for 5th Met) and expressed in tachyzoites. YFP labeling of *TgPyKII*2ndM-(19–357)-YFP-HA (Fig. 6B) and *TgPyKII*3rdM-(93–357)-YFP-HA (Fig. 6C) is localized only to the mitochondrion, whereas that of *TgPyKII*4thM-(122–357)-YFP-HA and *TgPyKII*5thM-(293–357)-YFP-HA is localized to cytosol (data not shown). These results suggest that the dual targeting of *TgPyKII*-1stM-(1–357)-YFP-HA could result from one protein product (*i.e.* 1st Met product targeted to both organelles) or two protein products (*i.e.* 1st Met product targeted to the apicoplast and either 2nd Met or 3rd Met product targeted to the mitochondrion). To determine whether there are one or two products responsible for the dual targeting, we performed site-directed mutagenesis changing 2nd Met or 3rd Met to Ala in *TgPyKII*1stM-(1–357)-YFP-HA construct and expressed them in tachyzoites. Although *TgPyKII*[2ndM19A]-YFP-HA targets YFP-HA to the apicoplast and the mitochondrion (Fig. 7A), *TgPyKII*[3rdM93A]-YFP-HA targeted only to the apicoplast (Fig. 7B). These results suggest that two protein products are responsible for dual targeting, 1st Met product for the apicoplast and the 3rd Met product for the mitochondrion.

DISCUSSION

We characterized a novel pyruvate kinase isozyme in *T. gondii*, *TgPyKII*, with unique enzymatic properties. pH optimum for *TgPyKII* activity is at 8.5, and more than 80% of the maximal activity was observed even at pH 9.0, more alkaline than the pH optima reported for any other pyruvate kinases (5.5–8.0) (42,

Novel Pyruvate Kinase in Two Organelles in *T. gondii*



FIGURE 4. Apicoplast and mitochondrial localization of native *TgPyKII* in *T. gondii* tachyzoite. Parasites stably expressing *ptubFNR₁-YFP-HA* (labeling apicoplast, green) were stained with MitoTracker Red CMXRos (red) and anti-*TgPyKII* antibody (blue). Note that in addition to apicoplast and mitochondrion, *TgPyKII* antibody localizes to apical ER (arrowheads) that may indicate a possible exit site of *TgPyKII* from ER. Scale bar, 5 μ m. DIC, differential interference contrast.

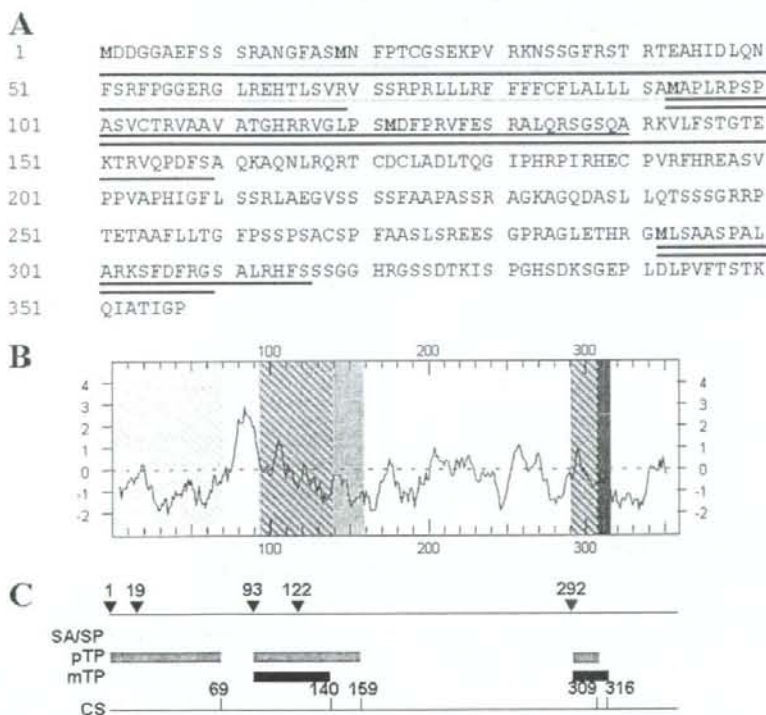


FIGURE 5. Signal prediction of the N-terminal extension of *TgPyKII* in *T. gondii*. **A**, N-terminal 357 amino acid sequence of *TgPyKII*. Methionines are highlighted in red. Colored underlines are location of predicted signals (see below for color codes). **B**, Kyte-Doolittle hydrophobicity plot of the N-terminal extension of *TgPyKII* showing a strong hydrophobic stretch between aa 75 and 92. Color-shaded regions are location of predicted signals (see below for color codes). Colors are hatched in regions where signals are overlapped. **C**, summary of predicted signals. Inverted black triangles indicate the location of each methionine with amino acid position listed above. The numbers above the tick mark indicate the amino acid position before the predicted signal cleavage sites. Colored boxes are location of predicted signals. Predicted SA/SP, orange; predicted plastid transit peptide (pTP), green; predicted mitochondrion targeting peptide (mTP), magenta; CS, cleavage site.

43). Although the actual physiological pH value of the apicoplast or the mitochondrion in *T. gondii* is still unknown, several enzymes localized in the apicoplast in *P. falciparum* (44), plastid in barley roots (45), or mitochondrion in yeast (46) and

Arabidopsis thaliana (47) have alkaline pH optima like *TgPyKII*. It is also possible, however, the maximal activity of *TgPyKII* may not be necessary in parasite survival.

Although ADP is generally considered as the phosphate recipient of pyruvate kinase in glycolysis, pyruvate kinase activity is relatively nonspecific in its utilization of purine and pyrimidine nucleotide substrates (48). Some bacterial pyruvate kinases prefer GDP over ADP (5, 49, 50), but their k_{cat}/K_m (or V_{max}/K_m) ratio for GDP is only 10–20-fold higher than that for ADP. However, in case of *TgPyKII*, GDP is preferred over ADP as a phosphate recipient with 377-fold higher k_{cat}/K_m (or V_{max}/K_m) ratio, suggesting GDP as a sole phosphate recipient.

Pyruvate kinases are generally activated by sugar phosphates and bind PEP allosterically (51). Albeit fructose 1,6-diphosphate is a typical allosteric activator, some pyruvate kinases use other activators such as fructose 2,6-diphosphate (52) in trypanosomatid protozoans and glucose 6-phosphate in *Eimeria tenella* (53), *Mycobacterium smegmatis* (54), *Streptococcus mutans* (49), and *TgPyK1* (11). Our study shows that *TgPyKII* is not activated by fructose 1,6-diphosphate and other known activators for pyruvate kinase such as sugar phosphates, and consistently, it does not show allosteric binding to PEP. Thus *TgPyKII* does not seem to have regulatory properties like as *TgPyK1*.

Pyruvate kinase can be classified by the requirement for a monovalent cation. Structural analysis (55), point mutation analysis (38, 39), and phylogenetic analysis (40) suggest that (Thr¹¹³ and Glu¹¹⁷) and (Leu/Ile¹¹³ and Ser/Lys¹¹⁷) (numbers in *F. catus* pyruvate kinase) are responsible for monovalent cation dependence and independence, respectively. Monovalent cation-independent isozymes (type II) exist in prokaryotes like actinobacteria, cyanobacteria, and proteobacteria, whereas monovalent cation-dependent isozymes (type I) exist in mammals, plants, and fungi (Fig. 2). In prokaryotes, *Clostridium perfringens*, *Leptospira interrogans*,

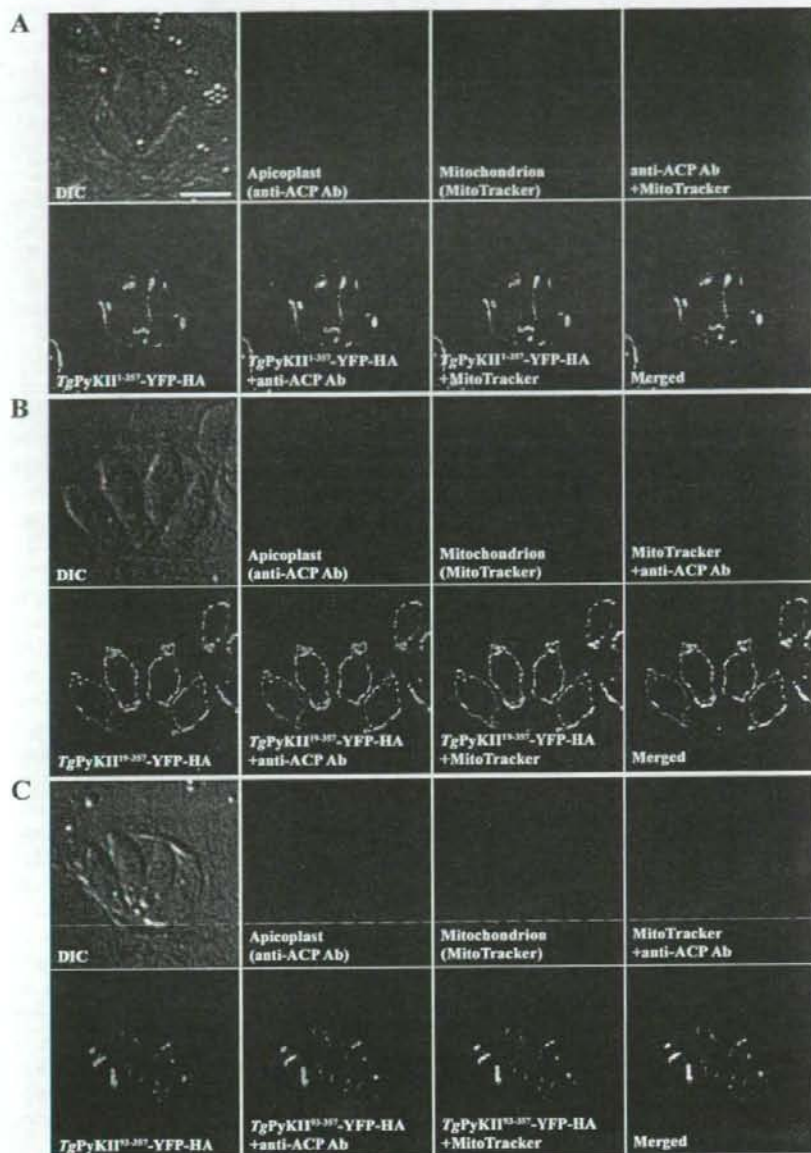


FIGURE 6. Localization of TgPyKII1stM-(1-357)-YFP-HA, TgPyKII2ndM-(19-357)-YFP-HA, and TgPyKII3rdM-(93-357)-YFP-HA. Parasites were transfected with TgPyKII1stM-(1-357)-YFP-HA (A), TgPyKII2ndM-(19-357)-YFP-HA (B), or TgPyKII3rdM-(93-357)-YFP-HA (C) under tubulin (in these panels) or dihydrofolate reductase (not shown) promoters and labeled with MitoTracker Red CMXRos (labeling mitochondrion, red) and anti-ACP antibody (labeling apicoplast, blue). The same phenotype was observed for different promoters. Scale bar, 5 μ m. DIC, differential interference contrast.

E. coli, *Vibrio cholerae*, and *Salmonella typhimurium* possess both types. In eukaryotes, so far only apicomplexan parasites, *T. gondii* (in this study), *P. falciparum* (56), *Theileria annulata* (contig 1823 and contig13), and *T. parva* (529.m04777 and 529.m0471) possess both types. Phylogenetic analysis shows that Apicomplexan type I pyruvate kinase clusters with plants and apicomplexan type II pyruvate kinase with proteobacteria (Fig. 2), suggesting that monovalent cation-independent

isozymes (type II) in apicomplexan parasites are of proteobacterial origin and obtained by horizontal gene transfer (Fig. 2). *Neospora caninum* possibly contains the proteobacteria-like pyruvate kinase isozyme (contig5134), but the full sequence has not been determined. The proteobacteria-like pyruvate kinase isozyme is not found in the complete genome sequence data base of *C. parvum*, which possesses a reduced mitochondria (mitome) but lacks the apicoplast. Genome sequencing of *Eimeria tenella* has not been completed at this time.

Another striking feature of TgPyKII is its dual localization to the apicoplast and mitochondrion as there is no documented evidence of a pyruvate kinase present in the mitochondrion in any other organism. In plants, although proteins are normally transported to chloroplasts or mitochondria from cytoplasm using organelle-specific N-terminal targeting signals, pTP or mTP, respectively, proteins can be dually targeted to both organelles by two types of signals as follows: (i) a twin presequence from alternative transcription start, alternative translation start, or alternative exons results in two proteins, one targeted to the chloroplast and the other to the mitochondrion; and (ii) an ambiguous presequence results in one protein targeted to both organelles (57). In *T. gondii*, although mitochondrial proteins use a classical mTP, proteins are targeted to the apicoplast, a secondary endosymbiotic plastid, using a unique N-terminal bipartite signal consisting of a secretory signal peptide (SP) followed by pTP (17, 58). Yet recently, a superoxide dismutase (TgSOD2) having a typical apicoplast bipartite signal is reported to localize to both apicoplast and mitochondrion as a single gene product (59). In this study, we showed that TgPyKII possesses an N-terminal extension, which contains five possible start codons and probable SA/SP, pTP, and mTP (Fig. 5). Using fluorescent reporter fused to N-terminal 357 aa from the 1st Met (TgPyKII1stM-(1-357)-YFP-HA), we prove that this region is responsible for localization to the apicoplast and the mitochondrion. Fluorescent fusions from 2nd and 3rd Met result in localization to the mito-

Novel Pyruvate Kinase in Two Organelles in *T. gondii*

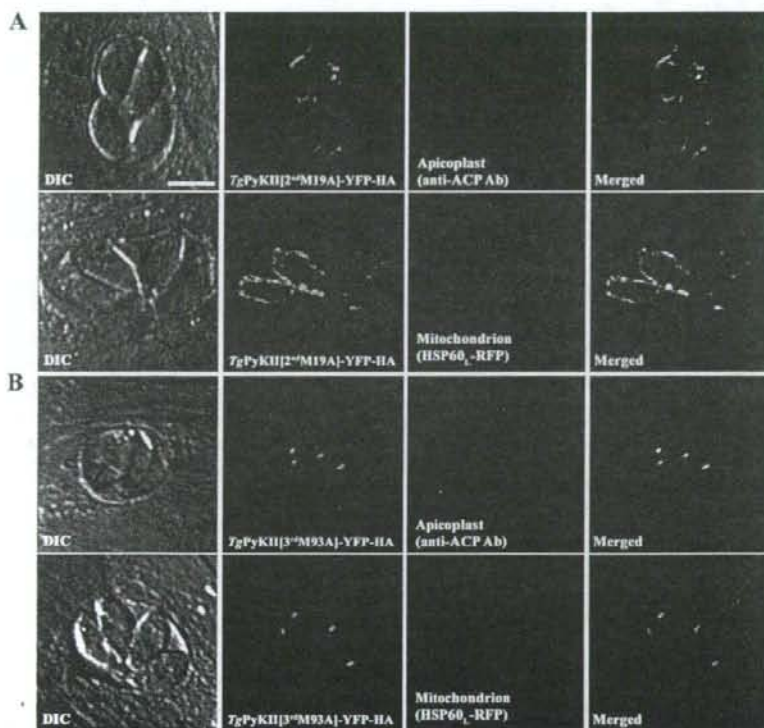


FIGURE 7. Localization of *TgPyKII*[2ndM19A]-YFP-HA and *TgPyKII*[3rdM93A]-YFP-HA. A, localization of *TgPyKII*[2ndM19A]-YFP-HA. Top panels, wild type RH parasites transfected with *pminTgPyKII*[2ndM19A]-YFP-HA (green) and labeled with anti-ACP antibody (labeling apicoplast, red). Bottom panels, RH parasites stably expressing HSP60_L-RFP (labeling mitochondrion, red) transfected with *pminTgPyKII*[2ndM19A]-YFP-HA (green). B, localization of *TgPyKII*[3rdM93A]-YFP-HA. Top panels, wild type RH parasites transfected with *pminTgPyKII*[3rdM93A]-YFP-HA (green) and labeled with anti-ACP antibody (labeling apicoplast, red). Bottom panels, RH parasites stably expressing HSP60_L-RFP (labeling mitochondrion, red) transfected with *pminTgPyKII*[3rdM93A]-YFP-HA (green). The same phenotype was observed for constructs under tubulin promoter. Scale bar, 5 μm. DIC, differential interference contrast.

chondrion only, suggesting that 1st Met product is responsible for apicoplast localization. *TgPyKII* was predicted to have an SA/SP (with higher probability for SA) from aa 1 to 92 (Fig. 5, *ocher*) because of an unusual hydrophobic region rich in leucine and phenylalanine between aa 75 and 92. However, *TgPyKII*[2ndM(19–357)]-YFP-HA, despite containing this hydrophobic region, does not localize to the apicoplast, suggesting that 18 aa between the 1st and 2nd Met is necessary for proper translocation into the ER and thus the apicoplast. Site-directed mutagenesis analysis showed that 3rd Met translation product, not 2nd Met, in the N-terminal extension of *TgPyKII* is responsible for the localization to the mitochondrion, consistent with the presence of mTP from 3rd Met (Fig. 5, *magenta*). Thus, unlike *TgSOD2*, two translation products are responsible for dual localization of *TgPyKII*, 1st Met product for the apicoplast and 3rd Met product for the mitochondrion. Further characterization of signals and signal cleavage sites has currently been carried out.

Type I monovalent cation-dependent isozymes in the apicomplexa lack an N-terminal extension, suggesting that, as in *TgPyKI*, they localize in the cytosol. On the other hand, type II monovalent cation-independent isozymes with proteobacterial

origin found in *P. falciparum*, *T. annulata*, and *T. parva* possess an N-terminal extension containing a typical bipartite apicoplast targeting signal. *P. falciparum* PyKII (AAN35560) does not have any internal methionines and was shown to localize only to the apicoplast by immunostaining using native antibody.⁶ *T. parva* PyKII (529.m04771) has internal methionines and could be dual-localized like as *TgPyKII*.

Although plant isozyme in plastids (60, 61) is a noncytosolic pyruvate kinase that functions in the glycolysis (62), noncytosolic pyruvate kinase found in the apicomplexan parasites may be involved in a unique metabolic pathway other than glycolysis, in which cytosolic pyruvate kinase plays a regulatory role. A plastidic sugar phosphate transporter was shown to localize to the apicoplast of *T. gondii* (16), which may suggest that triose sugars such as PEP could be transported from the cytosol to the apicoplast. Pyruvate dehydrogenase complex (59, 63, 64), enzymes in type II fatty acid synthesis (65, 66), and 1-deoxy-D-xylulose 5-phosphate synthesis (67) are localized in the apicoplast in *T. gondii*. Thus, in the apicoplast, *TgPyKII* may function in supplying acetyl Co-A in

cooperation with pyruvate dehydrogenase complex for fatty acid as well as 1-deoxy-D-xylulose 5-phosphate syntheses, as suggested in *P. falciparum* (68). Although *T. parva* does not possess FAS pathway in the apicoplast, PyKII in *T. parva* may contribute to the 1-deoxy-D-xylulose 5-phosphate pathway (69). The unique GTP supply role of *TgPyKII* may contribute to provide an energy source for protein synthesis and a substrate for RNA synthesis in the apicoplast that has its own DNA (70).

To date, pyruvate kinase has not been identified in the mitochondria of any organism. As the substrate PEP can be provided from gluconeogenesis pathway through mitochondrial PEP carboxykinase (NCBI ID BAC02911), this unusual "short cut" might contribute to the rapid switching from gluconeogenesis to the oxidative phosphorylation. However, the fate of the product pyruvate is currently unknown, as pyruvate dehydrogenase complex does not localize in the mitochondrion (59, 64), whereas *T. gondii* tricarboxylic acid cycle is functional in the tachyzoite stage (71–73). The metabolic pathway connecting pyruvate with tricarboxylic acid cycle in the mitochondria in

⁶ T. Maeda, T. Salto, O. Harb, D. S. Roos, A. Takeo, H. Suzuki, T. Tsuboi, T. Takeuchi, and T. Asai, unpublished data.

the apicomplexan parasites has been the unsolved question (34, 59, 63, 64). Although currently available data from biochemical and bioinformatics analyses do not provide explicit explanation for the role of TgPykII in the *T. gondii* mitochondrion, as the dual targeting to the apicoplast and mitochondrion can occur in previously unpredictable mechanisms in *T. gondii* (59 and in this study), further studies on experimental protein targeting may reconstruct metabolic pathways, and detailed information about the intraorganelle milieu will elucidate the physiological role of TgPykII in the mitochondrion.

REFERENCES

- Dubey, J. P. (1993) in *Parasitic Protozoa* (Kreier, J. P., ed) pp. 5–56. Academic Press, San Diego
- Fulton, J. D., and Spooner, D. F. (1960) *Exp. Parasitol.* **9**, 293–301
- Boyer, P. D. (1962) in *The Enzymes* (Boyer, P. D., Lardy, H., and Myrback, K., eds) 2nd Ed., pp. 95–113. Academic Press, New York
- Valentini, G., Chiarelli, L., Fortin, R., Speranza, M. L., Galizzi, A., and Mattevi, A. (2000) *J. Biol. Chem.* **275**, 18145–18152
- Waygood, E. B., and Sanwal, B. D. (1974) *J. Biol. Chem.* **249**, 265–274
- Waygood, E. B., Rayman, M. K., and Sanwal, B. D. (1975) *Can. J. Biochem.* **53**, 444–454
- Plaxton, W. C. (1996) *Annu. Rev. Plant Physiol. Plant Mol. Biol.* **47**, 185–214
- Saito, T., Maeda, T., Nakazawa, M., Takeuchi, T., Nozaki, T., and Asai, T. (2002) *Int. J. Parasitol.* **32**, 961–967
- Peng, Z. Y., and Mansour, T. E. (1992) *Mol. Biochem. Parasitol.* **54**, 223–230
- Denton, H., Roberts, C. W., Alexander, J., Thong, K. W., and Coombs, G. H. (1996) *FEMS Microbiol. Lett.* **137**, 103–108
- Maeda, T., Saito, T., Oguchi, Y., Nakazawa, M., Takeuchi, T., and Asai, T. (2003) *Parasitol. Res.* **89**, 259–265
- Bahl, A., Brunk, B., Crabtree, J., Fraunholz, M. J., Gajria, B., Grant, G. R., Ginsburg, H., Gupta, D., Kissinger, J. C., Labo, P., Li, L., Mailman, M. D., Milgram, A. J., Pearson, D. S., Roos, D. S., Schug, J., Stoeckert, C. J., Jr., and Whetzel, P. (2003) *Nucleic Acids Res.* **31**, 212–215
- Hoffman, S. L., Subramanian, G. M., Collins, F. H., and Venter, J. C. (2002) *Nature* **415**, 702–709
- Roos, D. S., Donald, R. G., Morrisette, N. S., and Moulton, A. L. (1994) *Methods Cell Biol.* **45**, 27–63
- Asai, T., and Suzuki, Y. (1990) *FEMS Microbiol. Lett.* **60**, 89–92
- Nishi, M. (2006) *Cell-cycle Regulation of Organelle Biogenesis and Apicoplast Protein Trafficking in Toxoplasma gondii*. Ph.D. thesis, University of Pennsylvania
- Waller, R. F., Keeling, P. J., Donald, R. G., Striepen, B., Handman, E., Lang-Unnasch, N., Cowman, A. F., Besra, G. S., Roos, D. S., and McFadden, G. I. (1998) *Proc. Natl. Acad. Sci. U.S.A.* **95**, 12352–12357
- Kissinger, J. C., Gajria, B., Li, L., Paulsen, I. T., and Roos, D. S. (2003) *Nucleic Acids Res.* **31**, 234–236
- Hulo, N., Bairoch, A., Bulliard, V., Cerutti, L., De Castro, E., Langendijk-Genevaux, P. S., Pagni, M., and Sigrist, C. J. (2006) *Nucleic Acids Res.* **34**, D227–D230
- Emanuelsson, O., Nielsen, H., Brunak, S., and von Heijne, G. (2000) *J. Mol. Biol.* **300**, 1005–1016
- Nielsen, H., Engelbrecht, J., Brunak, S., and von Heijne, G. (1997) *Protein Eng.* **10**, 1–6
- Bendtsen, J. D., Nielsen, H., von Heijne, G., and Brunak, S. (2004) *J. Mol. Biol.* **340**, 783–795
- Emanuelsson, O., Nielsen, H., and von Heijne, G. (1999) *Protein Sci.* **8**, 978–984
- Kyte, J., and Doolittle, R. F. (1982) *J. Mol. Biol.* **157**, 105–132
- Chen, F., Mackey, A. J., Stoeckert, C. J., Jr., and Roos, D. S. (2006) *Nucleic Acids Res.* **34**, D363–D368
- Li, L., Stoeckert, C. J., Jr., and Roos, D. S. (2003) *Genome Res.* **13**, 2178–2189
- Thompson, J. D., Gibson, T. J., Plewniak, F., Jeanmougin, F., and Higgins, D. G. (1997) *Nucleic Acids Res.* **25**, 4876–4882
- Felsenstein, J. (1989) *Cladistics* **5**, 164–166
- Schmidt, H. A., Strimmer, K., Vingron, M., and von Haeseler, A. (2002) *Bioinformatics (Oxf)* **18**, 502–504
- Huelsenbeck, J. P., and Ronquist, F. (2001) *Bioinformatics (Oxf)* **17**, 754–755
- Ronquist, F., and Huelsenbeck, J. P. (2003) *Bioinformatics (Oxf)* **19**, 1572–1574
- Kahn, A., and Marie, J. (1982) *Methods Enzymol.* **90**, 131–140
- Sibley, L. D., Niesman, I. R., Asai, T., and Takeuchi, T. (1994) *Exp. Parasitol.* **79**, 301–311
- van Dooren, G. G., Stimmier, L. M., and McFadden, G. I. (2006) *FEMS Microbiol. Rev.* **30**, 596–630
- Muirhead, H., Clayton, D. A., Barford, D., Lorimer, C. G., Fothergill-Gilmore, L. A., Schiltz, E., and Schmitt, W. (1986) *EMBO J.* **5**, 475–481
- Mattevi, A., Valentini, G., Rizzi, M., Speranza, M. L., Bolognesi, M., and Coda, A. (1995) *Structure (Lond.)* **3**, 729–741
- Rigden, D. J., Phillips, S. E., Michels, P. A., and Fothergill-Gilmore, L. A. (1999) *J. Mol. Biol.* **291**, 615–635
- Laughlin, L. T., and Reed, G. H. (1997) *Arch. Biochem. Biophys.* **348**, 262–267
- Jurica, M. S., Mesecar, A., Heath, P. J., Shi, W., Nowak, T., and Stoddard, B. L. (1998) *Structure (Lond.)* **6**, 195–210
- Oria-Hernandez, J., Riveros-Rosas, H., and Ramirez-Silva, L. (2006) *J. Biol. Chem.* **281**, 30717–30724
- Krogh, A., and Nielsen, H. (1998) in *Proceedings of the Sixth International Conference on Intelligent Systems for Molecular Biology (ISMB 6)*, Menlo Park, June 28–July 1, 1998, pp. 122–130. AAAI Press, Menlo Park, CA
- Saavedra, E., Olivos, A., Encalada, R., and Moreno-Sanchez, R. (2004) *Exp. Parasitol.* **106**, 11–21
- Hattori, J., Baum, B. R., McHugh, S. G., Blakeley, S. D., Dennis, D. T., and Miki, B. L. (1995) *Biochem. Syst. Ecol.* **23**, 773–780
- Dhanasekaran, S., Chandra, N. R., Chandrasekhar Sagar, B. K., Rangarajan, P. N., and Padmanaban, G. (2004) *J. Biol. Chem.* **279**, 6934–6942
- Esposito, S., Carfagna, S., Massaro, G., Vona, V., and Di Martino Rigano, V. (2001) *Planta* **212**, 627–634
- Jault, J. M., Di Pietro, A., Falson, P., and Gautheron, D. C. (1991) *J. Biol. Chem.* **266**, 8073–8078
- Olejnik, K., Murcha, M. W., Whelan, J., and Kraszewski, E. (2007) *FEBS J.* **274**, 4877–4885
- Plowman, K. M., and Krall, A. R. (1965) *Biochemistry* **4**, 2809–2814
- Abbe, K., and Yamada, T. (1982) *J. Bacteriol.* **149**, 299–305
- Crow, V. L., and Pritchard, G. G. (1982) *Methods Enzymol.* **90**, 165–170
- Munoz, M. E., and Ponce, E. (2003) *Comp. Biochem. Physiol. B. Biochem. Mol. Biol.* **135**, 197–218
- van Schaftingen, E., Vandercammen, A., Dethoux, M., and Davies, D. R. (1992) *Adv. Enzyme Regul.* **32**, 133–148
- Denton, H., Brown, S. M., Roberts, C. W., Alexander, J., McDonald, V., Thong, K. W., and Coombs, G. H. (1996) *Mol. Biochem. Parasitol.* **76**, 23–29
- Kapoor, R., and Venkatasubramanian, T. A. (1981) *Biochem. J.* **193**, 435–440
- Larsen, T. M., Laughlin, L. T., Holden, H. M., Rayment, I., and Reed, G. H. (1994) *Biochemistry* **33**, 6301–6309
- Gardner, M. J., Hall, N., Fung, E., White, O., Berriman, M., Hyman, R. W., Carlton, J. M., Pain, A., Nelson, K. E., Bowman, S., Paulsen, I. T., James, K. S., Eisen, J. A., Rutherford, K., Salzberg, S. L., Craig, A., Kyes, S., Chan, M. S., Nene, V., Shallom, S. J., Suh, B., Peterson, J., Angiuoli, S., Perlea, M., Allen, J., Selengut, J., Haft, D., Mather, M. W., Vaidya, A. B., Martin, D. M., Fairlamb, A. H., Fraunholz, M. J., Roos, D. S., Ralph, S. A., McFadden, G. I., Cummings, L. M., Subramanian, G. M., Mungall, C., Venter, J. C., Carucci, D. J., Hoffman, S. L., Newbold, C., Davis, R. W., Fraser, C. M., and Barrell, B. (2002) *Nature* **419**, 498–511
- Peeters, N., and Small, I. (2001) *Biochim. Biophys. Acta* **1541**, 54–63
- Roos, D. S., Crawford, M. J., Donald, R. G., Kissinger, J. C., Klimczak, L. J., and Striepen, B. (1999) *Curr. Opin. Microbiol.* **2**, 426–432
- Pino, P., Foth, B. J., Kwok, L. Y., Sheiner, L. S., Schepers, R., Soldati, T., and Soldati-Favre, D. (2007) *PLoS Pathog.* **3**, e115

Novel Pyruvate Kinase in Two Organelles in *T. gondii*

60. Ireland, R. J., Luca, V. D., and Dennis, D. T. (1979) *Plant Physiol.* **63**, 903–907
61. Ireland, R. J., Luca, V. D., and Dennis, D. T. (1980) *Plant Physiol.* **65**, 1188–1193
62. Simcox, P. D., and Dennis, D. T. (1978) *Plant Physiol.* **61**, 871–877
63. Foth, B. J., Stimmler, L. M., Handman, E., Crabb, B. S., Hodder, A. N., and McFadden, G. I. (2005) *Mol. Microbiol.* **55**, 39–53
64. Crawford, M. J., Thomsen-Zieger, N., Ray, M., Schachtner, J., Roos, D. S., and Seeber, F. (2006) *EMBO J.* **25**, 3214–3222
65. Jelenska, J., Crawford, M. J., Harb, O. S., Zuther, E., Haselkorn, R., Roos, D. S., and Gornicki, P. (2001) *Proc. Natl. Acad. Sci. U. S. A.* **98**, 2723–2728
66. Mazumdar, J., Wilson, E. H., Masek, K., Hunter, C. A., and Striepen, B. (2006) *Proc. Natl. Acad. Sci. U. S. A.* **103**, 13192–13197
67. Wiesner, J., and Seeber, F. (2005) *Expert Opin. Ther. Targets* **9**, 23–44
68. Ralph, S. A., Van Dooren, G. G., Waller, R. F., Crawford, M. J., Fraunholz, M. J., Foth, B. J., Tonkin, C. J., Roos, D. S., and McFadden, G. I. (2004) *Nat. Rev. Microbiol.* **2**, 203–216
69. Goodman, C. D., and McFadden, G. I. (2007) *Curr. Drug Targets* **8**, 15–30
70. Wilson, R. J., Denny, P. W., Preiser, P. R., Rangachari, K., Roberts, K., Roy, A., Whyte, A., Strath, M., Moore, D. J., Moore, P. W., and Williamson, D. H. (1996) *J. Mol. Biol.* **261**, 155–172
71. Coombs, G. H., Denton, H., Brown, S. M., and Thong, K. W. (1997) *Adv. Parasitol.* **39**, 141–226
72. Melo, E. J., Attias, M., and De Souza, W. (2000) *J. Struct. Biol.* **130**, 27–33
73. Vercesi, A. E., Rodrigues, C. O., Uyemura, S. A., Zhong, L., and Moreno, S. N. (1998) *J. Biol. Chem.* **273**, 31040–31047

Original Article

Seroprevalence of *Entamoeba histolytica* Infection in Female Outpatients at a Sexually Transmitted Disease Sentinel Clinic in Tokyo, Japan

Jun Suzuki*, Seiki Kobayashi¹, Ise Iku, Rie Murata, Yoshitoki Yanagawa and Tsutomu Takeuchi¹

Department of Microbiology, Tokyo Metropolitan Institute of Public Health, Tokyo 169-0073, and

¹Department of Tropical Medicine and Parasitology, School of Medicine, Keio University, Tokyo 160-8582, Japan

(Received December 13, 2007. Accepted February 19, 2008)

SUMMARY: From 2003 to 2006, we surveyed the seroprevalence of amoebic infection in female outpatients at a gynecologist's office, which was designated as a sexually transmitted disease sentinel clinic by the Tokyo Metropolitan Government, using an enzyme-linked immunosorbent assay (ELISA). The annual rate of anti-*Entamoeba histolytica* (HM-1:IMSSc16 strain; HM-1) antibody-positive cases as detected by ELISA increased during that period, and anti-*Chlamydia trachomatis* antibodies were detected in 60%, i.e., 24 of 40 anti-HM-1 antibody-positive individuals, suggesting sexual transmission of *E. histolytica*. We designed an ELISA with better sensitivity using the antigen extracted from the virulence-augmented *E. histolytica* strains (LHM-1 and LLA526 strains) by liver-passaging in hamsters. The average ratios of the S/N value (optical density [OD] of sample/OD of negative control) of ELISA with either the LHM-1 or LLA526 antigen and that of ELISA with the HM-1 antigen were significantly higher in intestinal amoebiasis cases with low S/N values than in amoebic liver abscess cases. In the present study of the seroprevalence of *E. histolytica* infection, the sera testing positive with low S/N values (<10) by ELISA with HM-1 antigen exhibited higher S/N values by ELISA using LHM-1 and LLA526 antigens. This modification of the antigen preparation for ELISA is expected to be effective in detecting anti-*E. histolytica* antibodies from such asymptomatic patients who have low antibody titers.

INTRODUCTION

In Japan, it was thought until the mid-1970s that amoebiasis was solely food borne and spread via food contaminated with cysts of *Entamoeba histolytica*. However, in the late 1970s, after amoebiasis was reported to have spread among men having sex with men (MSM) in large cities of the United States, it was recognized as a sexually transmitted disease (STD) (1,2). Within a few years, the suspected number of MSM having anti-*E. histolytica* antibodies along with anti-*Treponema pallidum* antibodies began to increase in densely populated cities in Japan (3,4).

In data provided by Japan's National Epidemiological Surveillance of Infectious Diseases, the number of notified cases with amoebiasis has been increasing annually; in 2006, 747 cases were reported, approximately 90% of which were male. However, with the spread of amoebiasis, the number of notified female cases has also increased at a slow but steady pace since 1999 (5,6).

In the present study, by detecting anti-*E. histolytica* (HM-1:IMSSc16 strain; HM-1) antibodies using an enzyme-linked immunosorbent assay (ELISA), we report the seroprevalence of amoebic infection in female outpatients who visited a gynecologist's office in Tokyo, Japan, from 2003 to 2006; this office was designated as an STD sentinel clinic by the Tokyo Metropolitan Government.

Moreover, in this study we attempted to design an ELISA with better sensitivity. This involved the use of the antigen

extracted from the virulence-augmented *E. histolytica* strains by liver-passaging in hamsters. The serum anti-*E. histolytica* antibody titers are low in a majority of asymptomatic amoebiasis cases. Practically, this serological method using LHM-1 and LLA526 antigens was tested on the anti-HM-1 antibody-positive sera in the present surveillance study.

MATERIALS AND METHODS

Study population: This study was conducted at a Tokyo gynecologist's office that was designated as an STD sentinel clinic by the Tokyo Metropolitan Government. We collected blood samples from 981 female outpatients between 2003 and 2006 (205 in 2003, 217 in 2004, 282 in 2005, and 277 in 2006) (Table 1). All individuals provided informed consent. Patient age was the only additional information. The anti-*E. histolytica* antibody-positive sera were examined for anti-*Chlamydia trachomatis* and anti-*T. pallidum* antibodies as indicators of STDs.

ELISA: *E. histolytica* antigens were prepared from axeni-

Table 1. Study samples in age categories from 2003 to 2006

Age	2003	2004	2005	2006	Total
<20	15	18	22	12	67
20-24	53	56	71	79	259
25-29	69	59	83	90	301
30-34	41	54	57	41	193
35-39	10	18	25	24	77
40-44	8	4	8	12	32
45-49	2	1	8	1	12
50<	1	2	5	7	15
unknown	6	5	3	11	25
Total	205	217	282	277	981

*Corresponding author: Mailing address: Division of Clinical Microbiology, Department of Microbiology, Tokyo Metropolitan Institute of Public Health, 3-24-1, Hyakunin-cho, Shinjuku-ku, Tokyo 169-0073, Japan. Tel: +81-3-3363-3231, Fax: +81-3-3368-4060, E-mail: Jun_Suzuki@member.metro.tokyo.jp

cally cultured *E. histolytica* (HM-1; ATCC no. 50527). The antigen was diluted with 0.05 M bicarbonate buffer to yield a concentration of 5 µg/mL. The diluted antigen (100 µL) was pipetted into each well of the microplate (Nunc-Immuno Module; Nunc Co., Roskilde, Denmark; Cat. no. 469078) and sensitized by incubation for 2 h at 37°C (7). After washing with a buffer (0.15 M phosphate buffer [PB] containing 0.05% Tween 20, pH 7.2; PB/T), 100 µL of the serum samples diluted 1:200 with a dilution buffer (PB/T containing 1% bovine serum albumin [BSA]) were pipetted into the microwells followed by incubation for 40 min at 37°C. The microplate was washed 3 times with PB/T after incubation, and 100 µL of 1:8,000 diluted peroxidase-conjugated anti-human IgG rabbit serum (ICN-Cappel Inc., Aurora, Ohio, USA; Cat. no. 55221) was added, followed by incubation for 40 min at 37°C. After washing with PB/T, the substrate solution comprising 0.03% 2,2'-azino-bis(3-ethylbenzothiazoline-6-sulfonic acid) diammonium salt (ABTS; Sigma Co., St. Louis, Mo., USA; Cat. no. A1888), 0.01% H₂O₂ in 10 mL of 0.1 M Na₂HPO₄, and 10 mL of 0.1 M citric acid was added to each well. After 7 min, 50 µL of 1.25% NaF solution was added to arrest color development, and an ELISA reader (MTP-120) (Corona Electric Co., Ltd., Ibaragi, Japan) was used to measure the absorbance at 405 nm. The cut-off S/N optical density (OD) value, calculated using the average OD of negative sera from 5 healthy individuals, was set at 3.

Serological test for *C. trachomatis* and *T. pallidum* infections: Anti-*C. trachomatis* IgG and IgA antibodies were measured using a solid-phase enzyme immunoassay kit (Peptide-Chlamydia IgG and IgA; Ani Labsystems Ltd., Oy, Vantaa, Finland).

Nontreponemal anti-cardiolipin (CL) antibodies were detected using two kits (biologic false-positive tests for syphilis), i.e., slide test antigen (DS Pharma-Biomedicals, Osaka, Japan) and rapid plasma reagin (RPR) test (Sanko Junyaku, Tokyo, Japan). The sera that tested positive by these kits were retested using the *T. pallidum* passive hemagglutination (TPHA) kit (Fujirebio, Inc., Tokyo, Japan) for detection of anti-*T. pallidum* antibody. The OD values of the positive and negative control sera for quality control and the OD value of the positive control of the kits were measured during each run of all the serological tests.

ELISA with antigens from virulence-augmented amoebae: Based on the hypothesis that the amount of antigenic substances would also decrease simultaneously with the loss of virulence, we attempted to design an ELISA with better sensitivity in the following manner: (i) HM-1 and LA526 strains cultured axenically for 3 days in the TYI-S-33 medium were inoculated (dose, 1 × 10⁶ amoebae/0.1 mL/head) into the left hepatic lobes of female Syrian golden hamsters (age, 3–4 weeks) (8). (ii) On the 6th day of inoculation, the hamsters were sacrificed and the livers dissected aseptically. The amoebic abscesses isolated from each of the livers were minced finely and crushed using scissors for medical use in the TYI-S-33 medium (9). (iii) After removing the tissue debris from the amoebic cell suspensions and washing twice in the TYI-S-33 medium by centrifugation (175 × g for 3 min), both *E. histolytica* strains were cultured axenically in the TYI-S-33 medium. They were named LHM-1 and LLA526. The long-term axenically cultured HM-1 was passaged 16 times through hamster liver due to the significant reduction in virulence, whereas the LA526 was passaged only once because it was newly isolated from the pus of a human amoebic liver abscess only 8 months earlier. (iv) LHM-1 and LLA526

were mass cultured within 2 weeks after their transfer into TYI-S-33 medium from the amoebic liver abscesses. The antigens were then harvested and washed twice in phosphate buffered saline (PBS) by centrifugation (175 × g for 3 min) and suspended in 5 mL of distilled water, followed by intermittent sonication (UH-150; SMT Co., Ltd., Tokyo, Japan) at 10 kHz for 5 min in an ice bath. (v) The sonicated suspensions were then centrifuged at 9,100 × g for 30 min, and the protein concentrations of the aqueous soluble extracts were measured by Bradford's method (10). (vi) LHM-1 and LLA526 antigens were sensitized at a concentration of 0.5 µg/well according to the procedures described above.

Each serum sample was tested in triplicate for each of the three antigens—LHM-1, LLA526, and HM-1—and the average OD values were calculated. The sensitivity of ELISA for each of the three antigens was compared with the positive serum samples of 5 patients clinically diagnosed having amoebic liver abscesses and 5 mentally handicapped persons in a rehabilitation institution for the intellectually impaired in Japan, who were almost free from amoebiasis symptoms but positive for *E. histolytica* cysts on microscopy and for *E. histolytica* antigen when tested by using an *E. histolytica*-specific antigen detection kit (*E. histolytica* II kit; TechLab, Blacksburg, Va., USA). In each of the 10 human serum samples obtained as described above from the cases of amoebic liver abscess and asymptomatic cyst passers, the ratio was determined between the S/N values (OD value of serum sample [S]/average OD of negative sera from 5 healthy individuals [N]) of ELISA with the LHM-1 and HM-1 antigens and that between the S/N values of ELISA with the LLA526 and HM-1 antigens.

RESULTS

Seroprevalence of anti-*E. histolytica* antibodies in the female population: During the 4 years 2003 to 2006, in the 981 sera samples obtained from the study population, the seroprevalence of anti-*E. histolytica* (HM-1) antibodies increased every year. In 2005 and 2006, the annual positive rate was >5%; the average annual positive rate over the 4 years was 4.1% (40/981) (Table 2). In addition, 60%, i.e., 24/40 of these cases, were also positive for anti-*C. trachomatis* antibodies—an indicator of STDs. On the other hand, none of the cases were positive for anti-CL antibodies (a retest by the TPHA kit was not performed). The strong positive correlation between seropositivity for anti-*E. histolytica* and anti-*C. trachomatis* antibodies suggested sexual transmission of *E. histolytica* in the female population. The age range with the highest number of individuals positive for anti-*E. histolytica* antibodies was that of 25–29 years, with 11, and that of 30–

Table 2. Seroprevalence of anti-*Entamoeba histolytica* antibodies in the female outpatients from a gynecologist's office, Tokyo, Japan, by enzyme-linked immunosorbent assay from 2003 to 2006

Year	No. of samples	No. of positives	Positive rate %	No. of positives for anti-CT antibodies ¹⁾
2003	205	3	1.5	2
2004	217	8	3.7	6
2005	282	14	5.0	7
2006	277	15	5.4	9
Total	981	40	4.1	24

¹⁾ Number of positives for anti-*Chlamydia trachomatis* (CT) antibodies that were also positive for anti-*E. histolytica* antibodies.

Table 3. Age distribution of the female outpatients from a gynecologist's office with positive for anti-*Entamoeba histolytica* antibodies

Year	20-24	25-29	30-34	35-39	40-44	45-49	50<
2003	1	1 (1)		1 (1)			
2004		2 (1)	3 (3)	2 (2)			
2005	1	2 (1)	3 (1)		3	4 (3)	2 (2)
2006	3 (2)	6 (5)	3 (2)		2		1
Total	5 (2)	11 (8)	9 (6)	3 (3)	5	4 (3)	3 (2)

Number of positives for anti-*Chlamydia trachomatis* antibodies that were also positive for anti-*E. histolytica* antibodies are provided in parentheses.

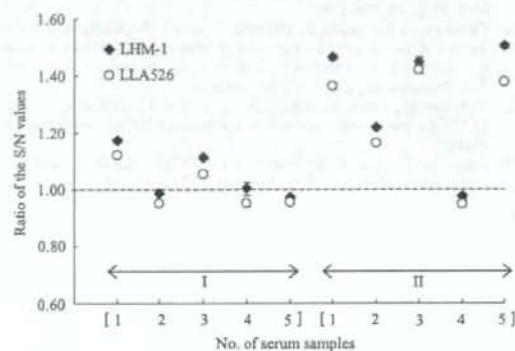


Fig. 1. Ratio of the S/N values of ELISA with better sensitivity performed using the antigens from hamster liver-passaged LHM-1 and LLA526 strains to the S/N values of ELISA using the antigen from the HM-1:IMSSc16 (HM-1) strain in the clinical serum samples of amoebiasis (S/N values: OD of serum sample [S]/average OD of negative sera [N]). The mean of the ratios of triplicate ELISA are plotted. I: Samples ($n = 5$); anti-HM-1 antibody-positive sera from the clinical patients of amoebic liver abscess. The S/N values of ELISA with LHM-1 and LLA526 antigens did not increase significantly ($P > 0.05$ by t test). II: Samples ($n = 5$); anti-HM-1 antibody-positive sera from the mentally handicapped individuals admitted to a rehabilitation institution for the intellectually impaired in Japan. The S/N values of ELISA with LHM-1 and LLA526 antigens increased significantly ($P < 0.05$ by t test).

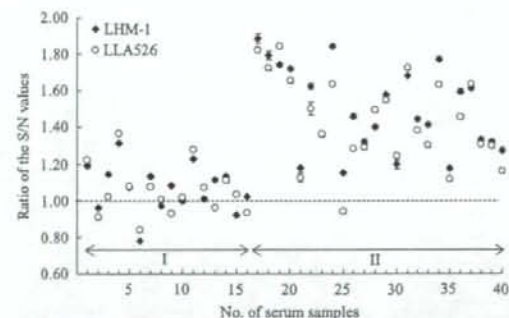


Fig. 2. Ratio of S/N values of ELISA performed using antigens from the LHM-1 and LLA526 strains to the S/N values of conventional ELISA performed using the antigen from the HM-1 strain in female outpatients from a gynecologist's office. The mean of the ratios of triplicate ELISA are plotted. I: Samples ($n = 16$); anti-HM-1 antibody-positive sera with high S/N values (≥ 10). The S/N values of ELISA with LHM-1 and LLA526 antigens did not increase significantly ($P > 0.05$ by t test). II: Samples ($n = 24$); anti-HM-1 antibody-positive sera with low S/N values (< 10). The S/N values by ELISA with LHM-1 and LLA526 antigens increased significantly ($P < 0.01$ by t test).

34 years, with 9. The number of individuals positive for anti-*C. tracomatis* antibodies correlated with the number of those positive for anti-*E. histolytica* antibodies (Table 3).

Comparison of S/N values of ELISA with three different antigens: Figure 1 shows the results of a pilot study in which ELISA with LHM-1 and LLA526 antigens was conducted using sera from 5 human cases each of amoebic liver abscess and asymptomatic cyst passers. The average ratio (1.324) between S/N values of ELISA with the LHM-1 and HM-1 antigens and that (1.254) between S/N values of ELISA with the LLA526 and HM-1 antigens increased significantly only in asymptomatic cases with low S/N values ($P < 0.05$ by t test) and not in amoebic liver abscess cases (1.048 and 1.006, respectively; $P > 0.05$ by t test).

The 40 anti-HM-1 antibody-positive sera as detected by ELISA were classified into two groups based on the magnitude of the S/N values (i.e., groups I and II with S/N values ≥ 10 and < 10 , respectively). The tendency of ELISA with LHM-1 and LLA526 antigens to yield significantly higher S/N values ($P < 0.01$ by t test) was also confirmed in seropositive cases from among the present study population with low S/N values (< 10) by ELISA using the HM-1 antigen (Figure 2).

DISCUSSION

In Japan, the MSM population is still thought to be a major high-risk group for STDs. However, our study provided evidence indicating that the seroprevalence of the *E. histolytica* infection in the female population of Tokyo is increasing annually.

In addition, the result that 60% of the female study population who were anti-*E. histolytica* antibody-positive were also positive for anti-*C. tracomatis* antibodies, an indicator of STD, along with the diversity of sexual behavior suggested that a major proportion of females positive for anti-*E. histolytica* antibodies may have been infected with *E. histolytica* by sexual transmission. We do not fully understand why none of the cases were positive for anti-CL antibodies in the female population, unlike the case in the MSM population (11,12). We are currently conducting further epidemiological studies on the route of *E. histolytica* infection in the female population.

The tendency of ELISA using the LHM-1 and LLA526 antigens to yield statistically higher S/N values ($P < 0.01$ by t test) was evident only in the positive cases with low S/N values (< 10) among the present female study population. The active antigenic substance that brought about this effect could not be identified in the present study. Despite the necessity of further evaluation, the improved ELISA is expected to be effective for detecting anti-*E. histolytica* antibodies from such asymptomatic patients who have low antibody titers. Moreover, the hamster liver-passaged *E. histolytica* may be applied as a sensitive antigen to other serodiagnostic methods, such as dot-ELISA (13) and immunofluorescence antibody tests (14).

Because of the public's indifference to STDs, the control of amoebiasis should start with efforts to raise public awareness of the risk of infection by sexual transmission. Also simpler and more sensitive mass examination methods should be developed, such as the newly designed ELISA using the antigen extracted from the virulence-augmented *E. histolytica* strains, which have a better sensitivity for the diagnosis of amoebiasis.

ACKNOWLEDGMENTS

A part of this work was supported by a Health Sciences Research Grant-in-Aid for Emerging and Re-emerging Infectious Diseases from the Ministry of Health, Labour and Welfare of Japan.

REFERENCES

1. Markell, E.K., Havens, R.F., Kuritsubo, R.A., et al. (1984): Intestinal protozoa in homosexual men of the San Francisco Bay area: prevalence and correlates of infection. *Am. J. Trop. Med. Hyg.*, 33, 239-245.
2. Schmerin, M.J., Gelston, A. and Jones, T.C. (1977): Amebiasis. An increasing problem among homosexuals in New York City. *JAMA*, 238, 1386-1387.
3. Takeuchi, T., Okuzawa, E., Nozaki, T., et al. (1989): High seropositivity of Japanese homosexual men for amebic infection. *J. Infect. Dis.*, 159, 808.
4. Nozaki, T., Motta, S.R., Takeuchi, T., et al. (1989): Pathogenic zymodemes of *Entamoeba histolytica* in Japanese male homosexual population. *Trans. R. Soc. Trop. Med. Hyg.*, 83, 525.
5. National Institute of Infectious Diseases and Tuberculosis and Infectious Diseases Control Division, Ministry of Health, Labour and Welfare (2007): Amebiasis in Japan, 2003-2006. *Infect. Agents Surveillance Rep.*, 28, 103'-104'.
6. Infectious Disease Surveillance Center, National Institute of Infectious Diseases: Annual Data Summary. Online at <<http://idsc.nih.gov/jp/idwr/>

ydata/index-e.html>.

7. Kanwar, J.R. and Vinayak, V.K. (1991): A comparative efficacy of plate ELISA and dot ELISA to detect antiamebic antibodies in clinical patients. *Trop. Geogr. Med.*, 43, 261-265.
8. Diamond, L.S., Phillips, B.P. and Bartgis, I.L. (1974): A comparison of the virulence of nine strains of axenically cultivated *E. histolytica* in hamster liver. *Arch. Invest. Med.*, 5, 423-426.
9. Diamond, L.S., Harlow, D.R. and Cunnick, C.C. (1978): A new medium for the axenic cultivation of *Entamoeba histolytica* and other *Entamoeba*. *Trans. R. Soc. Trop. Med. Hyg.*, 72, 431-432.
10. Bradford, M.M. (1976): A rapid and sensitive method for the quantitation of microgram quantities of protein utilizing the principle of protein-dye binding. *Anal. Biochem.*, 72, 248-254.
11. Takeuchi, T., Kobayashi, S., Asami, K., et al. (1987): Correlation of positive syphilis serology with invasive amebiasis in Japan. *Am. J. Trop. Med. Hyg.*, 36, 321-324.
12. Okusawa, E., Kobayashi, S., Miyahira, Y., et al. (1991): Study on clinical forms and demographic backgrounds of Japanese adult males with invasive amebiasis according to the history of sexual practice. *Jpn. Arch. Sex. Transm. Dis.*, 1, 153-156 (in Japanese).
13. Yamaura, H., Araki, K., Kiuchi, K., et al. (2003): Evaluation of dot-ELISA for serological diagnosis of amebiasis. *J. Infect. Chemother.*, 9, 25-29.
14. Ambrose-Thomas, P. and Truong, T.K. (1972): Fluorescent antibody test in amebiasis. *Am. J. Trop. Med. Hyg.*, 21, 907-912.

Critical role of dendritic cells in determining the T_H1/T_H2 balance upon *Leishmania major* infection

Kazutomo Suzue^{1,2}, Seiki Kobayashi³, Tsutomu Takeuchi³, Mamoru Suzuki² and Shigeo Koyasu^{1,4}

¹Department of Microbiology and Immunology, Keio University School of Medicine, 35 Shinanomachi, Shinjuku-ku, Tokyo 160-8582, Japan

²Department of Parasitology, Gunma University Graduate School of Medicine, 3-39-22 Showa-machi, Maebashi, Gunma 371-8511, Japan

³Department of Tropical Medicine and Parasitology, Keio University School of Medicine, 35 Shinanomachi, Shinjuku-ku, Tokyo 160-8582, Japan

⁴Core Research for Evolutional Science and Technology, Japan Science and Technology Corporation, Kawaguchi 332-0012, Japan

Keywords: antigen-presenting cell, infectious disease, protozoan parasite, T_H

Abstract

The onset of T_H1 immunity is in part regulated by genetic background. To elucidate the cell type carrying critical factors determining the T_H1 response, we employed Rag-2^{-/-} mice on *Leishmania major*-susceptible BALB/c and -resistant B10.D2 backgrounds. By using bone marrow (BM) chimeras generated by the transplantation of B10.D2 BM cells into BALB/c-Rag-2^{-/-} mice, and *vice versa*, it was shown that hematopoietic cells carry factors determining the disease outcome and T_H1 response against *L. major* infection. B10.D2-Rag-2^{-/-} mice reconstituted with BALB/c CD4⁺ T cells exhibited a T_H1 response and controlled *L. major* infection. Wild-type BALB/c mice inoculated with *L. major*-parasitized B10.D2-Rag-2^{-/-} splenocytes also exhibited a T_H1 response and a mild disease outcome, whereas such a T_H1 response was not induced when CD11c⁺ dendritic cells (DCs) were depleted from parasitized B10.D2-Rag-2^{-/-} splenocytes. T_H1 response was reconstituted by the addition of *L. major*-parasitized B10.D2 DCs but not *L. major*-parasitized BALB/c DCs to DC-depleted parasitized B10.D2-Rag-2^{-/-} splenocytes. These results indicate that DCs determine the outcome of the disease upon *L. major* infection.

Introduction

The balance between two distinct CD4⁺ T_H responses, namely T_H1 and T_H2 immune responses, is tightly correlated with the outcome of various diseases including tumor, auto-immune diseases and infectious diseases (1). Understanding the basis of the genetic control of T_H1/T_H2 differentiation is important for the development of vaccines and therapeutic strategies. The infection of mice with *Leishmania major*, a macrophage-tropic intracellular protozoan parasite, is widely employed as a model for the functional analyses of T_H1 and T_H2 responses upon microbial infection (2). After infection with *L. major*, most strains of wild-type (WT) mice exhibit a T_H1 immune response that is essential in controlling the intracellular micro-organism. In contrast, BALB/c mice exhibit a T_H2 response and succumb to *L. major* infection (2–4).

Previous studies have reported that a fraction of CD4⁺ T cells recognizing a specific *Leishmania* antigen produce a large amount of IL-4 during the early phase of infection in

naive BALB/c mice (5, 6). Such IL-4 production is considered to be the exacerbation factor of *L. major* infection by instructing naive T cells to elicit a T_H2 response in BALB/c mice (6–8). On the other hand, other reports have shown that B10.D2 mice also produce a large amount of IL-4 but are able to control *L. major* infection and BALB.B mice sharing the same MHC with C57BL/6 and C57BL/10 mice produce only a small amount of IL-4 yet succumb to infection (9, 10). In addition, BALB/c mice mount a T_H2 response upon infection with *L. major* lacking an immunodominant epitope that induces early IL-4 production from CD4⁺ T cells (11). Furthermore, IL-4-deficient mice on a BALB/c background are still susceptible to *L. major* (12). These findings suggest that cells other than the specific subset of T cells producing IL-4 are crucial in determining the outcome of *L. major* infection in BALB/c mice.

To this end, we performed a series of experiments to determine the cell type carrying the genetic factors that

controls the outcome of the disease upon *L. major* infection by using Rag-2^{-/-} mice on *L. major*-susceptible BALB/c and -resistant B10.D2 backgrounds. Our results demonstrate that dendritic cells (DCs) play a critical role in determining the T_H1/T_H2 balance as well as the outcome of disease upon *L. major* infection.

Methods

Mice

WT BALB/c and B10.D2 mice were purchased from Japan SLC (Shizuoka, Japan) and Rag-2^{-/-} mice on BALB/c (N12) and B10.D2 (N10) backgrounds (13, 14) were obtained from Taconic (Germantown, NY, USA). Mice were maintained in our specific pathogen-free facility and all experiments were performed in accordance with our Institutional Guidelines.

Antibodies

FITC-, PE- and biotin-labeled mAbs were purchased from BD PharMingen (San Diego, CA, USA). FITC-F4/80 and Red670-streptavidin were purchased from Caltag Laboratories (Burlingame, CA, USA) and GIBCO BRL (Grand Island, NY, USA), respectively. All magnetic bead-conjugated mAbs were purchased from Miltenyi Biotec (Sunnyvale, CA, USA).

Leishmania major infection

Leishmania major (MHOM/SU/73/5-ASKH) was maintained in BALB/c mice. Before experiments, parasites were obtained from the infection site on a left hind footpad and promastigotes were propagated at 26°C in Schneider's *Drosophila* medium (GIBCO BRL) containing 15% heat-inactivated FCS. Mice were subcutaneously injected with 5×10^6 of stationary-phase promastigotes at left hind footpads. In some experiments, mice were injected with 1×10^7 of promastigote-parasitized splenocytes from Rag-2^{-/-} mice.

The severity of the disease was evaluated by the footpad swelling and parasite burdens in the infected footpads and, in some experiments, popliteal lymph nodes. The footpad thickness was measured with a vernier caliper and the swelling caused by infection was determined by subtracting the thickness of the uninfected right hind footpad from that of the infected left hind footpad. To determine parasite burdens, infected footpads and/or popliteal lymph nodes were homogenized with steel mesh and 5-fold serially diluted with 15% FCS-containing Schneider's *Drosophila* medium and incubated at 26°C for 14 days. Emerged promastigotes were monitored and the parasite burden was calculated by the last dilution of promastigotes emerged (15).

Cell preparation

To obtain bone marrow (BM) cells, cells were prepared aseptically from femora. After removing RBCs by treatment with ammonium chloride solution, BM cells (2×10^7 cells ml^{-1}) were washed and suspended in PBS. To obtain splenocytes, spleen was first digested by injection of collagenase D solution (Boehringer Mannheim, Indianapolis, IN, USA) with a 26-G needle. After 10-min incubation at 37°C, spleen was minced with forceps. After pipetting, cell suspension was filtrated with nylon mesh to remove connective

tissues. To obtain naive CD4⁺ T cells from splenocytes, B and CD8⁺ T cells were initially removed by using anti-CD8 and anti-B220 magnetic bead-conjugated mAbs. CD4⁺ T cells were then positively collected with anti-CD4-conjugated magnetic beads and AutoMACS (Miltenyi Biotec) in accordance with the manufacturer's protocols. Purity of CD4⁺ T cells was >95% in all experiments. Splenic DCs were obtained by magnetic separation of CD11c⁺ cells from Rag-2^{-/-} splenocytes. To obtain bone marrow-derived dendritic cells (BMDCs), BM cells from Rag-2^{-/-} mice were cultured in RPMI 1640 medium supplemented with 10% FCS, penicillin and streptomycin, 10 mM HEPES and 200 U ml^{-1} of granulocyte macrophage colony-stimulating factor (PeproTech, London, UK). Ten days after culture, non-adherent cells were collected and CD11c⁺ DCs were positively collected by magnetic sorting with AutoMACS. Purity of CD11c⁺ cells was >90%.

In vitro parasitization

To prepare parasitized cells, Rag-2^{-/-} splenocytes or BMDCs were mixed with *L. major* promastigotes (cells:promastigotes = 3:1) and incubated for 2 h at 37°C with rotation, washed three times to exclude extracellular promastigotes and suspended in PBS. To prepare DC-removed parasitized Rag-2^{-/-} splenocytes, parasitized cells were mixed with anti-CD11c magnetic beads and CD11c⁺ DCs were removed with VarioMACS (Miltenyi Biotec) in accordance with the manufacturer's protocols. Over 95% of CD11c⁺ cells were removed from parasitized Rag-2^{-/-} splenocytes. In some experiments, DC-removed parasitized Rag-2^{-/-} splenocytes were mixed with parasitized CD11c⁺ DCs at a ratio of 4:1 (determining by the percentage of CD11c⁺ cells in Rag-2^{-/-} splenocytes). To confirm the rate of parasitization, amastigotes in parasitized cells were directly observed on thin-blood smear specimens by Giemsa staining 3 days after parasitization. The infection rates of BALB/c and B10.D2 cells were nearly the same through all the experiments (data not shown).

T_H1/T_H2 cytokine assay

To determine the T_H1/T_H2 balance in mice, 4.0×10^5 splenocytes (2.0×10^6 ml^{-1}) were stimulated with freeze-thaw killed leishmanial antigens. Two days after stimulation, culture supernatants were harvested and stored at -80°C until performing ELISA. All ELISAs were performed with OptEIA™ ELISA sets (BD PharMingen) in accordance with the manufacturer's protocols.

Statistics

Student's *t*-test was applied to the results of footpad swelling and Mann-Whitney's *U*-test was applied to the results of parasite burdens.

Results

Genetic background of BM cells determines the outcome of *L. major* infection

To examine whether the outcome of *Leishmania* infection is determined by hematopoietic or non-hematopoietic cells, we

employed BM chimeras using Rag-2^{-/-} mice on *L. major*-susceptible BALB/c and -resistant B10.D2 backgrounds. Rag-2^{-/-} mice were lethally irradiated and transplanted with BM cells from BALB/c or B10.D2 WT mice. Two months after the transplantation of BM cells when the proportion of peripheral leukocytes was nearly the same as WT mice, BM chimeras were infected with *L. major*. As shown in Fig. 1, the outcome of infection such as footpad swelling, parasite burden and T_H1/T_H2 balance were reflected on the genetic background of BM donor. B10.D2-Rag-2^{-/-} mice transplanted with BALB/c BM cells were unable to control *L. major* infection as revealed by progressive footpad swelling and high parasite burden in infected footpads as compared with the mice transplanted with B10.D2 BM cells (Fig. 1A and B). Moreover, these chimeras exhibited a T_H2 response as shown by the production of a small amount of IFN- γ and a large amount of IL-4 from splenocytes by re-stimulation with *L. major* antigens (Fig. 1C). In contrast, the BM chimeras based on BALB/c-Rag-2^{-/-} mice transplanted with B10.D2 BM cells efficiently controlled the infection (Fig. 1D and E) and exhibited a characteristic T_H1 response (Fig. 1F) as compared with the mice transplanted with BALB/c BM cells. These results indicate that BM cells carry genetic factors controlling *L. major* infection.

Genetic background of CD4⁺ T cells is minimally involved with the outcome

Next, to examine whether the outcome of *L. major* infection is determined by the genetic background of CD4⁺ T cells (6), Rag-2^{-/-} mice were reconstituted with CD4⁺ T cells from naive B10.D2 or BALB/c WT mice and infected with *L. major*. B10.D2-Rag-2^{-/-} mice reconstituted with CD4⁺ T cells from either B10.D2 or BALB/c mice exhibited milder symptoms as compared with BALB/c-Rag-2^{-/-} mice reconstituted with BALB/c CD4⁺ T cells (Fig. 2). The ratios of IFN- γ and IL-4 produced by splenocytes were similar in B10.D2-Rag-2^{-/-} mice reconstituted with B10.D2 and BALB/c CD4⁺ T cells. On the other hand, such ratio was lower in BALB/c-Rag-2^{-/-} mice reconstituted with BALB/c CD4⁺ T cells. These results indicate that the outcome of disease is largely dependent upon the genetic background of recipient Rag-2^{-/-} mice and, more specifically, non-T and -B cells among BM-derived cells.

Cells that first encounter parasites determine the outcome of infection

It has been suggested that the outcome of the disease upon infection with *L. major* is determined at an early phase of infection (7, 8). For example, the administration of cytokines or neutralizing antibodies against cytokines during the early phase of infection can drastically alter the disease outcome (7, 8). We therefore hypothesized that cells that initially encounter parasites determine the outcome of *L. major* infection. To examine the hypothesis, Rag-2^{-/-} splenocytes containing macrophages and DCs were mixed with *L. major* promastigotes *in vitro* and parasitized cells were subcutaneously inoculated into the footpad of WT mice. Since macrophages are the major reservoir of *Leishmania* (2), leishmaniasis is induced by the inoculation of parasitized Rag-2^{-/-} splenocytes.

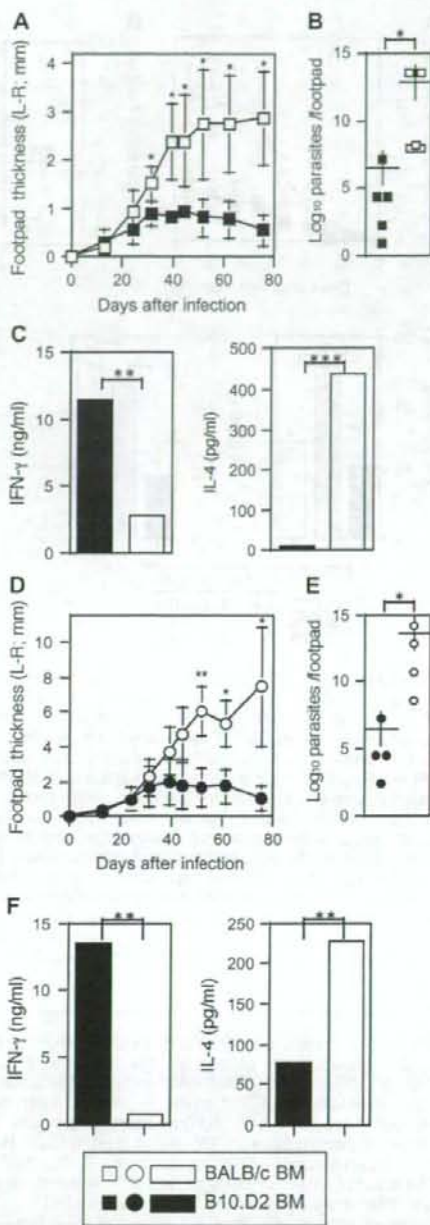


Fig. 1. The outcome of *Leishmania major* infection on BM chimeras is determined by the genetic background of BM cell donor. B10.D2-Rag-2^{-/-} (A-C) and BALB/c-Rag-2^{-/-} (D-F) mice were irradiated at 9 and 6 Gy, respectively, and reconstituted with 10⁷ B10.D2-WT (closed symbols and bars) or BALB/c-WT BM (open symbols and bars) cells. Two months after transplantation, mice were administered with *L. major* promastigotes at left hind footpads. (A and D) Footpad swelling caused by *L. major* infection. (B and E) Parasite burdens in infected footpads. +, mean of each group. (C and F) IFN- γ and IL-4 production by splenocytes induced by parasite antigens. *P < 0.01, **P < 0.001 and ***P < 0.0001.